

Electronic Supplementary Information

A combined theoretical and experimental approach to determine the right choice of co-ligand to impart spin crossover in Fe(II) complexes based on 1,3,4-Oxadiazole ligands

Sriram Sundaresan,^a Julian Eppelsheimer,^a Esha Gera,^b Lukas Wiener,^a Luca M Carrella, Kuduva R. Vignesh,^{b,*} and Eva Rentschler^{a,*}

^aDepartment Chemie, Johannes-Gutenberg-Universität Mainz, Duesbergweg 10–14, 55128 Mainz, Germany. Email: rentschl@uni-mainz.de

^bDepartment of Chemical Sciences, Indian Institute of Science Education Research (IISER) Mohali, Sector-81, Knowledge City, S.A.S. Nagar, Mohali-140306, Punjab, India. Email: vigneshkuduvar@iisermohali.ac.in

Contents

1. NMR Spectra	2
2. IR Spectra	7
3. Crystal data:	11
4. Cyclic Voltammetry:	31
5. Solid-State Magnetic Data:	32
6. Computational details:	34
7. References	37

1. NMR Spectra

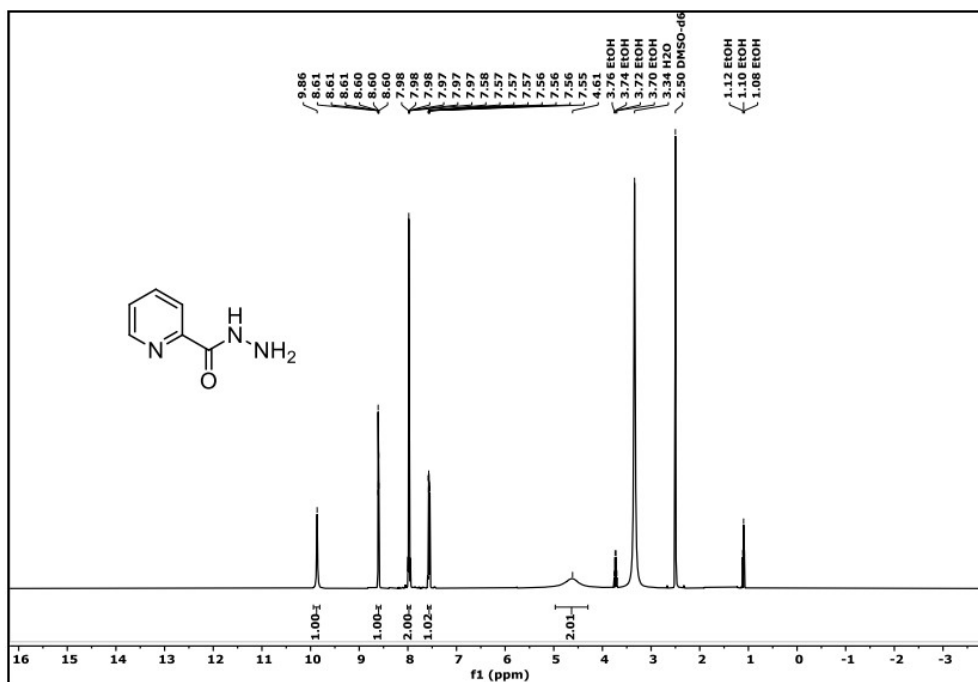


Figure S1: $^1\text{H-NMR}$ spectrum of Pyridine-2-carboxylic acid hydrazide in DMSO.

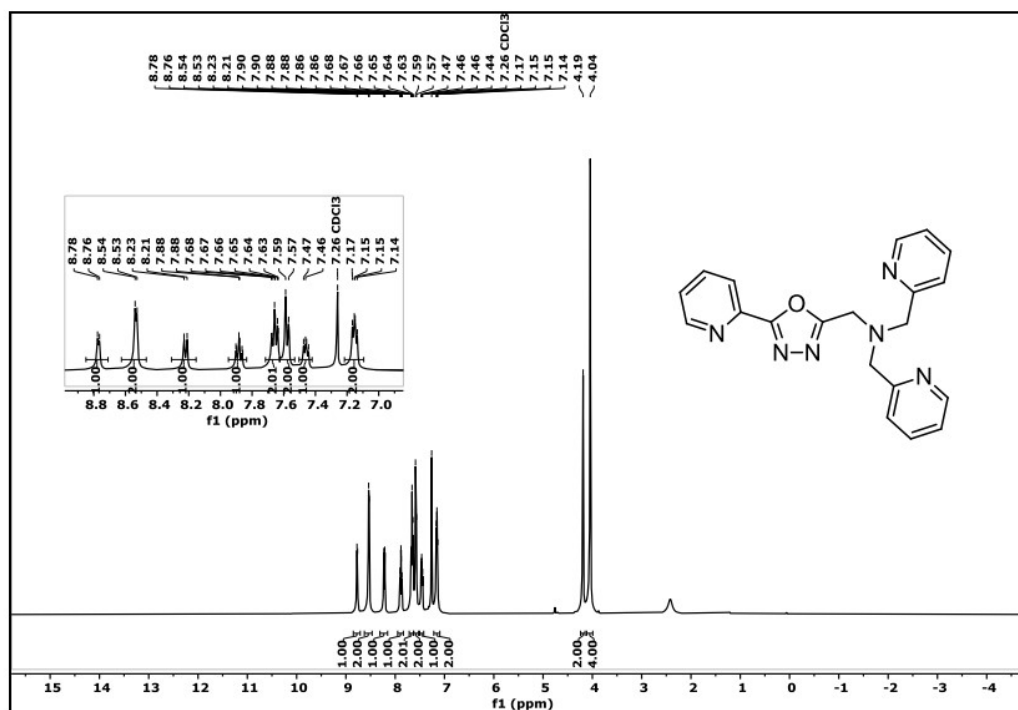


Figure S2: $^1\text{H-NMR}$ spectrum of 2-(2-Pyridyl)-5-[N,N-bis(2-pyridylmethyl)aminomethyl]-1,3,4-oxadiazole (**L**_{TetraPy-ODA}) in CDCl_3 .

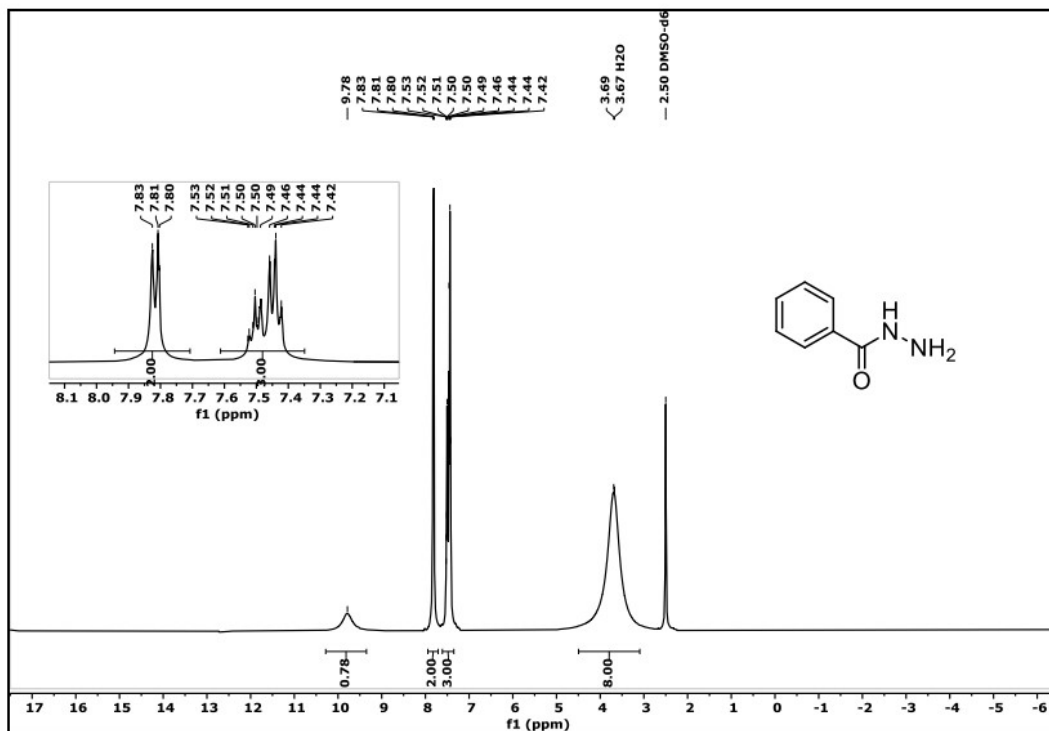


Figure S3: ¹H-NMR spectrum of Benzoic acid hydrazide in DMSO.

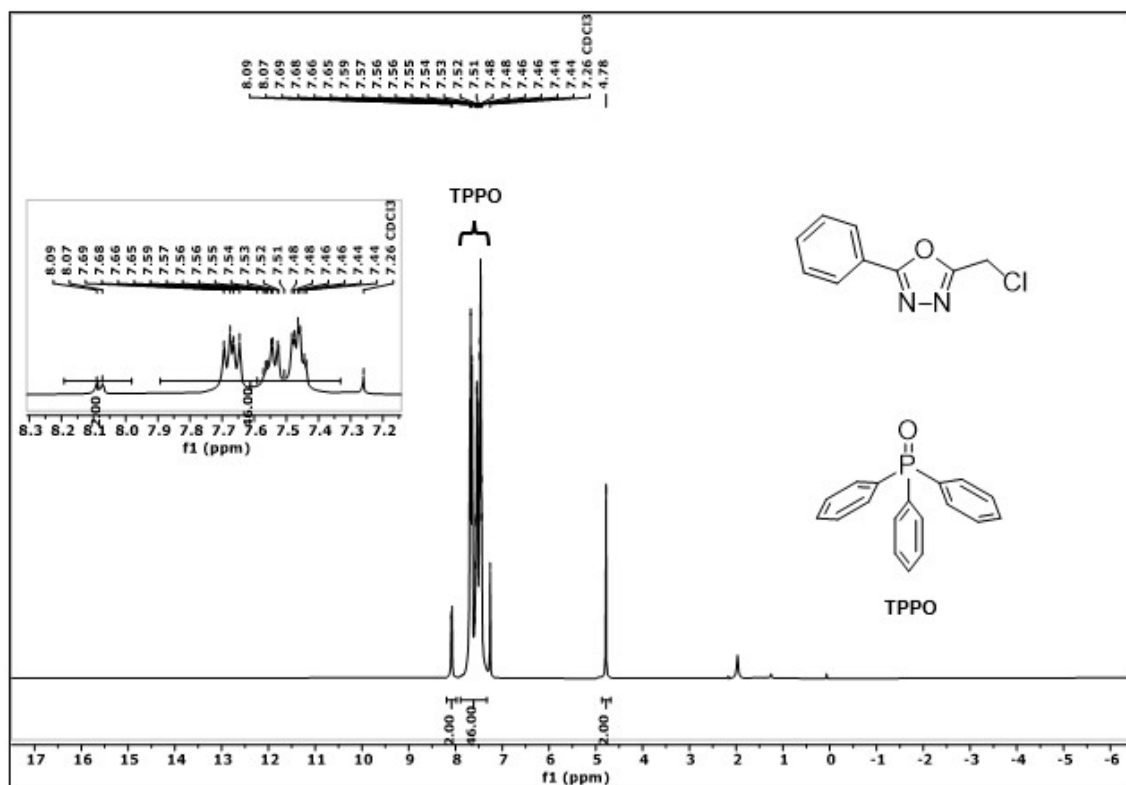


Figure S4: ¹H-NMR spectrum of 2-(Chloromethyl)-5-phenyl-1,3,4-oxadiazole and TPPO in CDCl₃

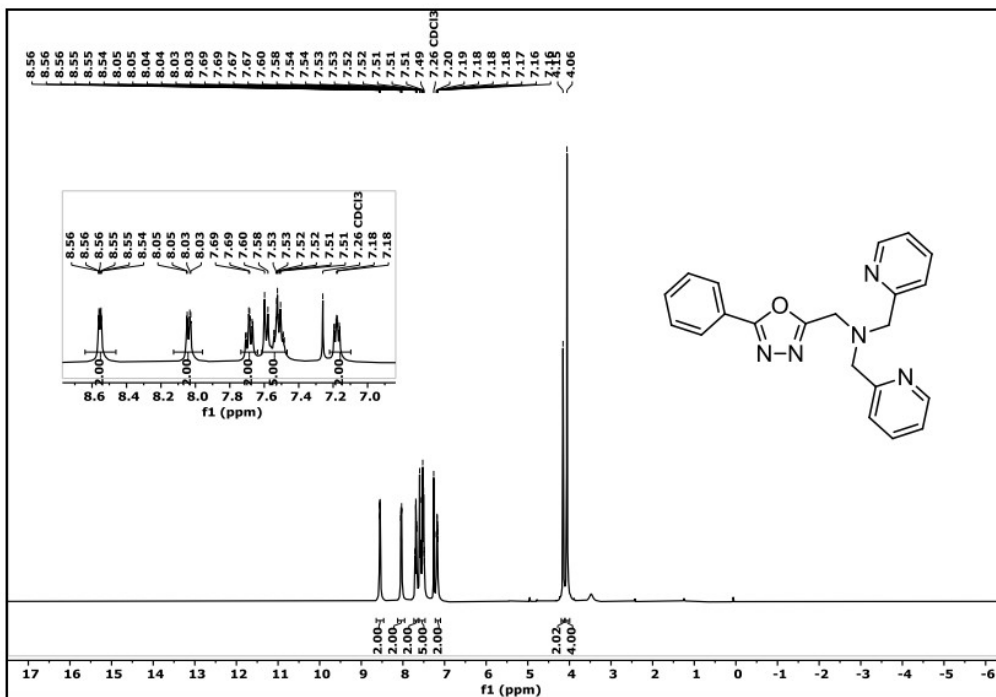


Figure S5: ¹H-NMR spectrum of 2-Phenyl-5-[N,N-bis(2-pyridylmethyl)aminomethyl]-1,3,4-oxadiazole (**L**^{TetraPh}-ODA) in CDCl₃.

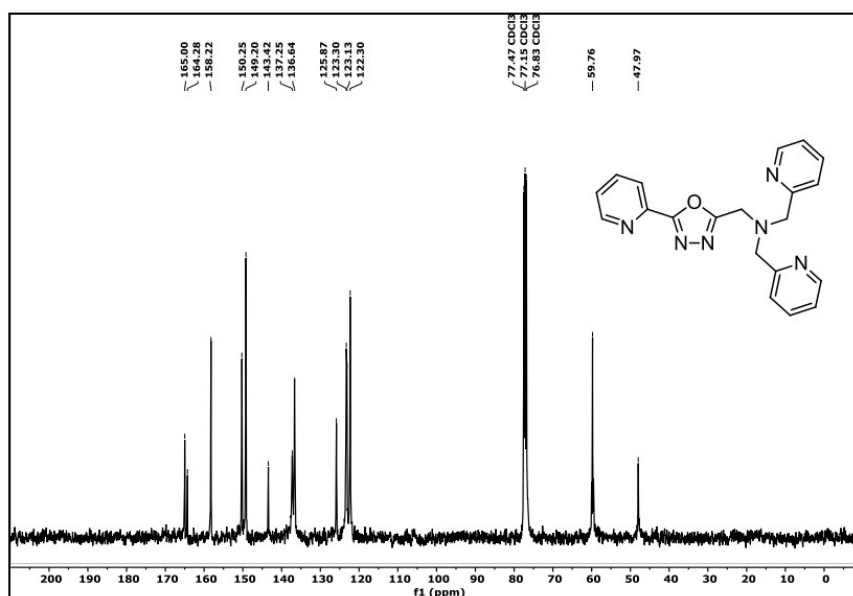


Figure S6: ¹³C-NMR spectrum of 2-(2-Pyridyl)-5-[N,N-bis(2-pyridylmethyl)aminomethyl]-1,3,4-oxadiazole (**L**^{TetraPy}-ODA) in CDCl₃.

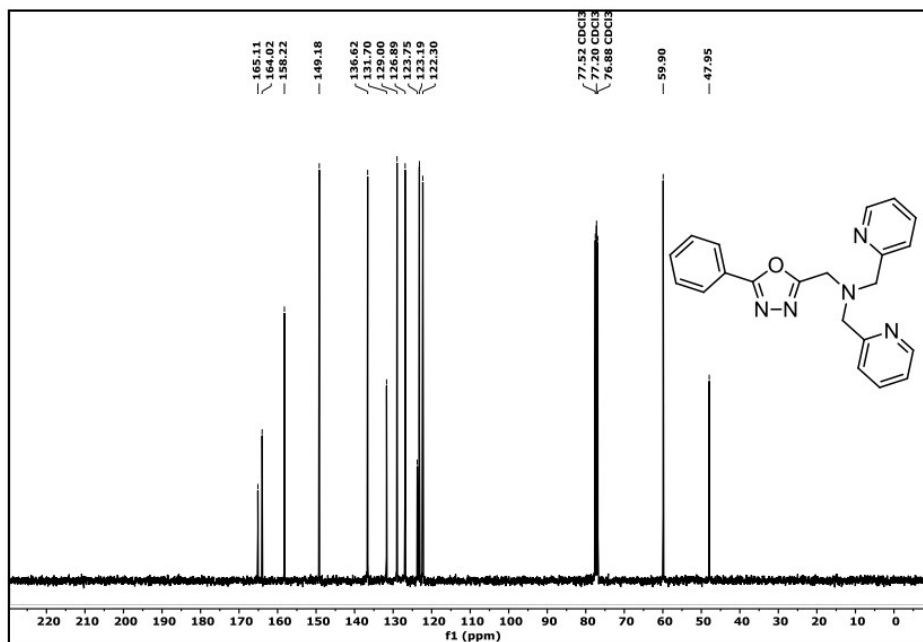


Figure S7: ^{13}C -NMR spectrum of 2-Phenyl-5-[N,N-bis(2-pyridylmethyl)aminomethyl]-1,3,4-oxadiazole ($\text{L}^{\text{TetraPh-ODA}}$) in CDCl_3 .

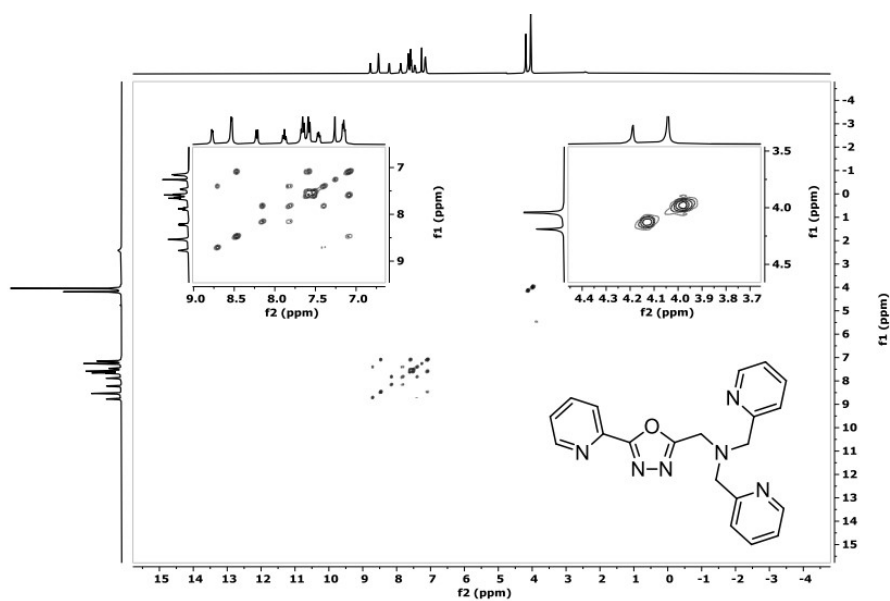


Figure S8: ^1H - ^1H -COSY spectrum of 2-(2-Pyridyl)-5-[N,N-bis(2-pyridylmethyl)aminomethyl]-1,3,4-oxadiazole ($\text{L}^{\text{TetraPy-ODA}}$) in CDCl_3 .

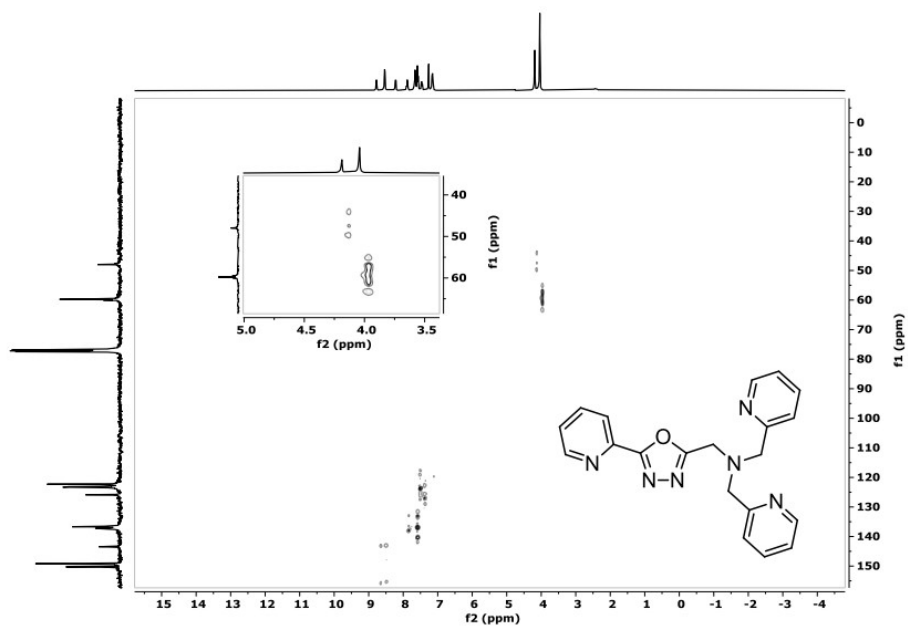


Figure S9: ^1H - ^{13}C -HSQC spectrum of 2-(2-Pyridyl)-5-[N,N-bis(2-pyridylmethyl)aminomethyl]-1,3,4-oxadiazole ($\text{L}_{\text{TetraPy-ODA}}$) in CDCl_3 .

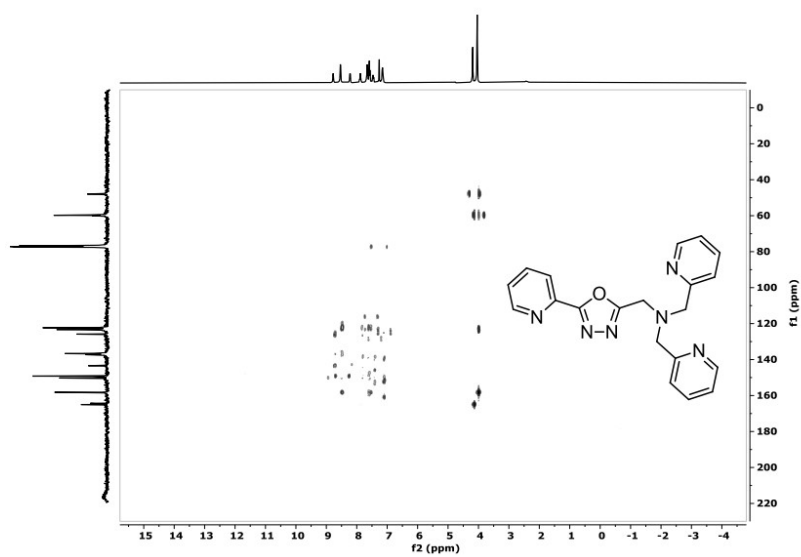


Figure S10: ^1H - ^{13}C -HMBC spectrum of 2-(2-Pyridyl)-5-[N,N-bis(2-pyridylmethyl)aminomethyl]-1,3,4-oxadiazole ($\text{L}_{\text{TetraPy-ODA}}$) in CDCl_3 .

2. IR Spectra

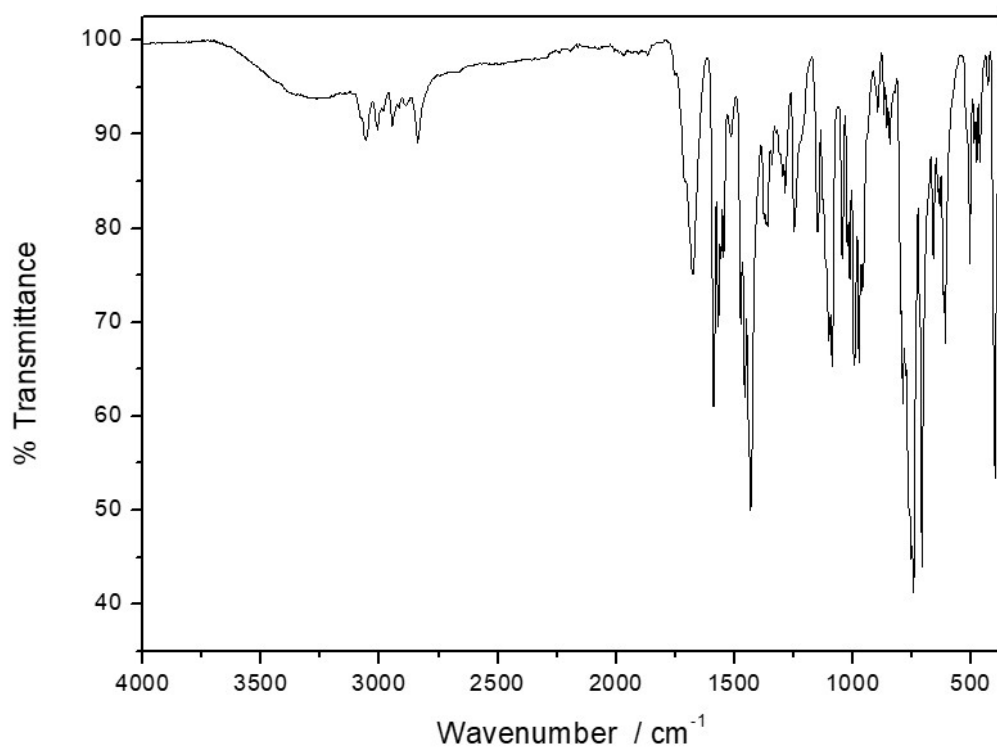


Figure S11: IR spectrum of 2-(2-Pyridyl)-5-[N,N-bis(2-pyridylmethyl)aminomethyl]-1,3,4-oxadiazole ($L^{\text{TetraPy-ODA}}$).

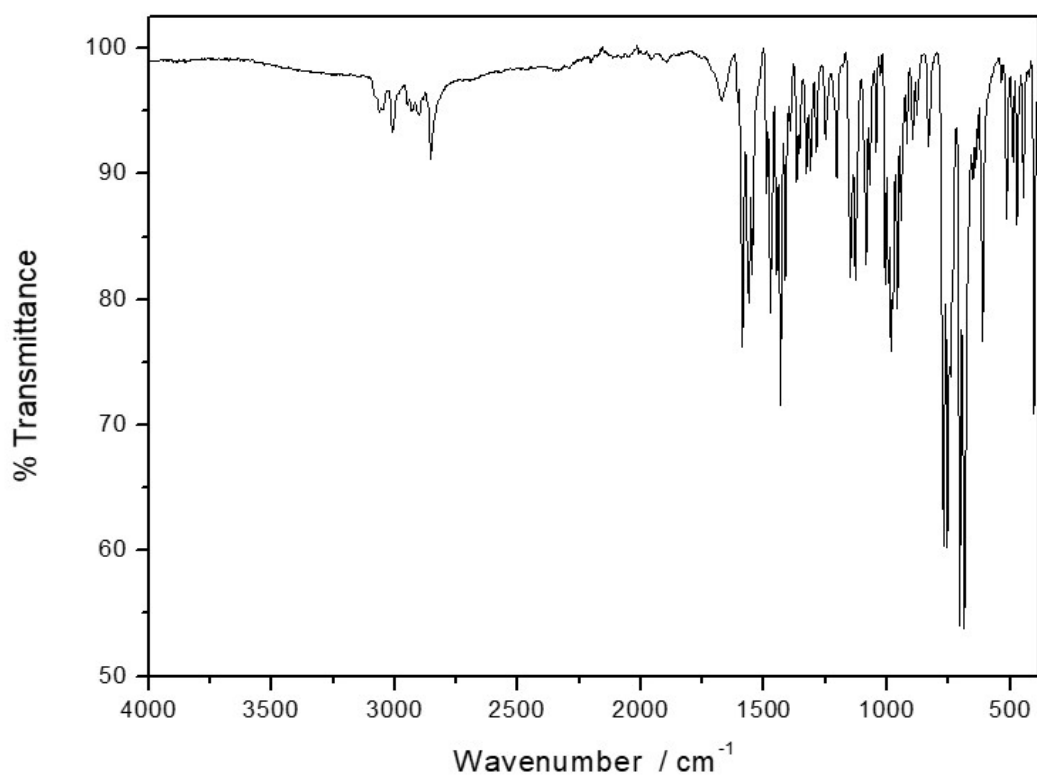


Figure S12: IR spectrum of 2-Phenyl-5-[N,N-bis(2-pyridylmethyl)aminomethyl]-1,3,4-oxadiazole ($L^{\text{TetraPh-ODA}}$).

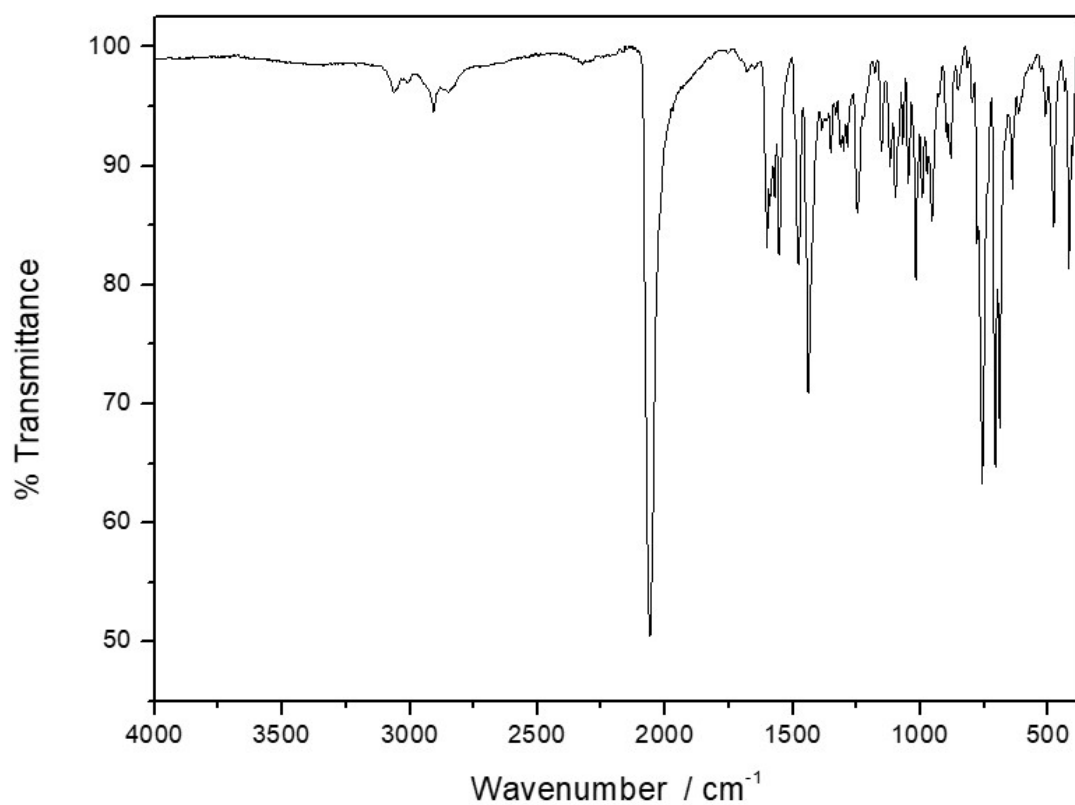


Figure S13: IR spectrum of $[\text{Fe}^{\text{II}}(\text{L}^{\text{TetraPh-ODA}})(\text{NCS})]$ (C4).

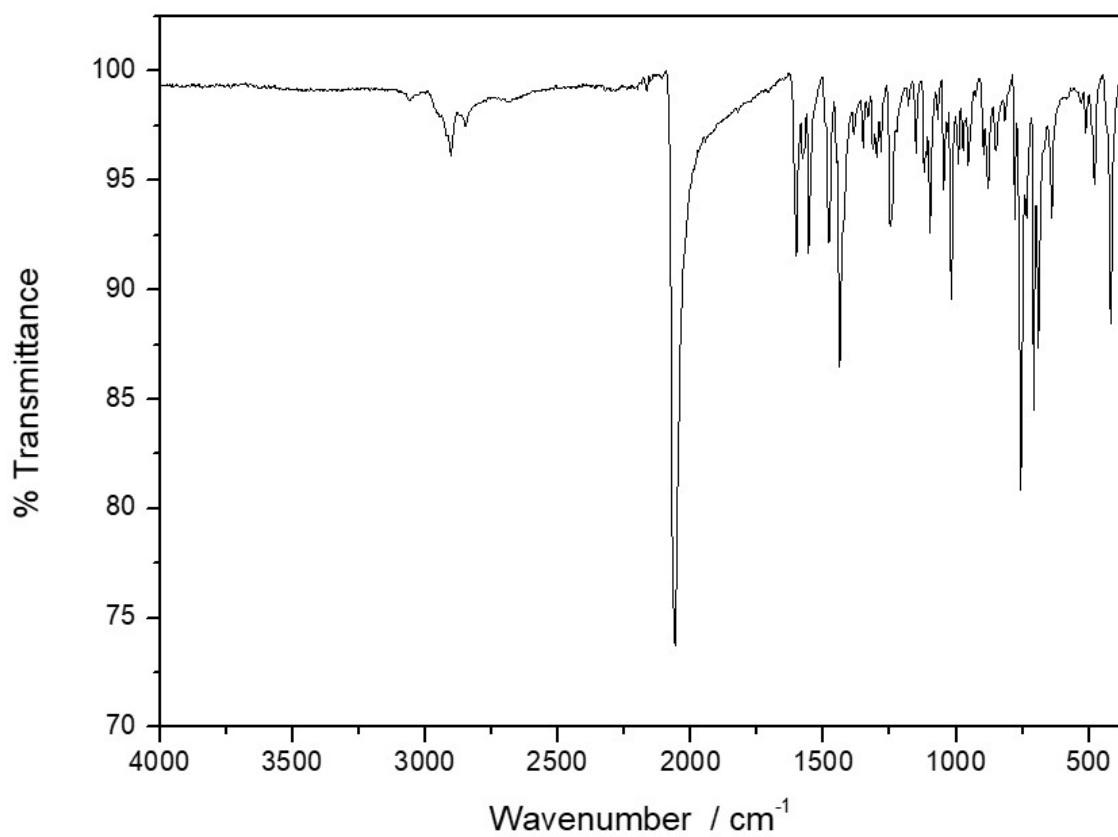


Figure S14: IR spectrum of $[\text{Fe}^{\text{II}}(\text{L}^{\text{TetraPh-ODA}})(\text{NCSe})]$ (C5).

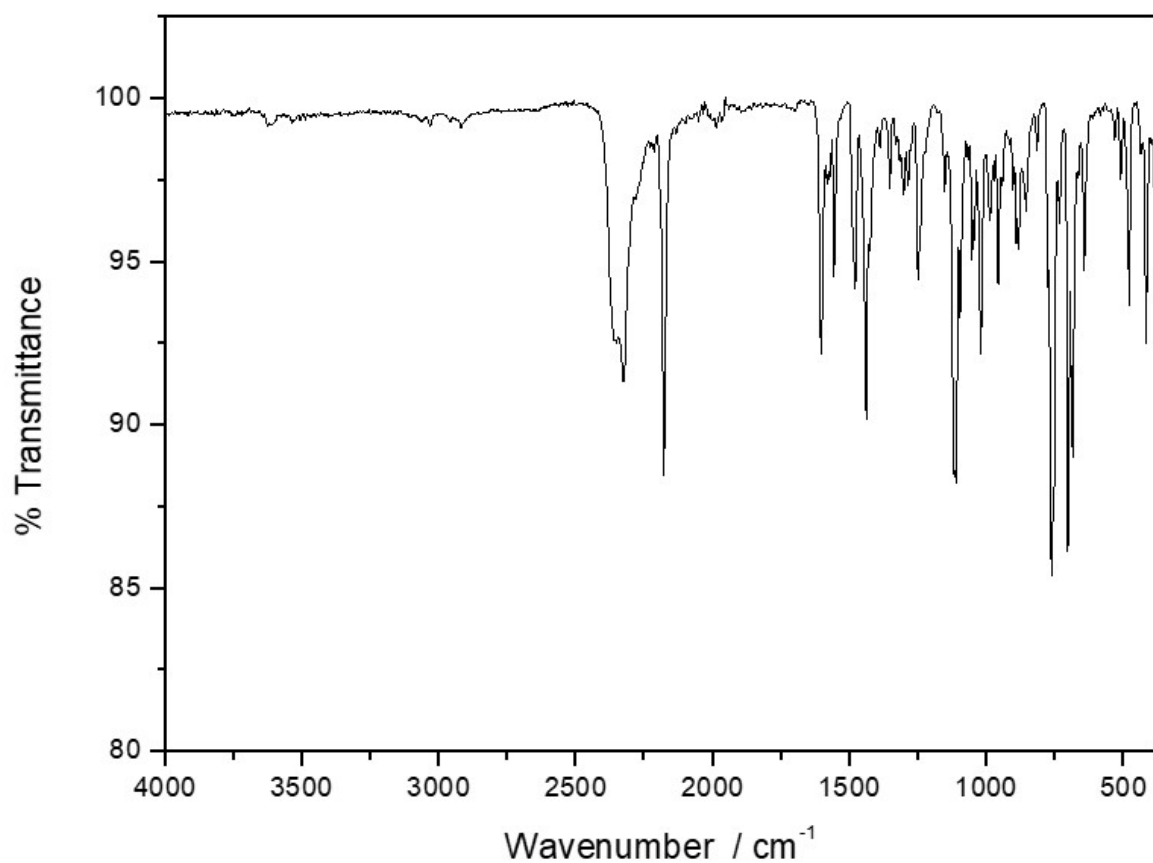


Figure S15: IR spectrum of [Fe^{II}(L^{TetraPh-ODA})(NCBH₃)₂] (C6).

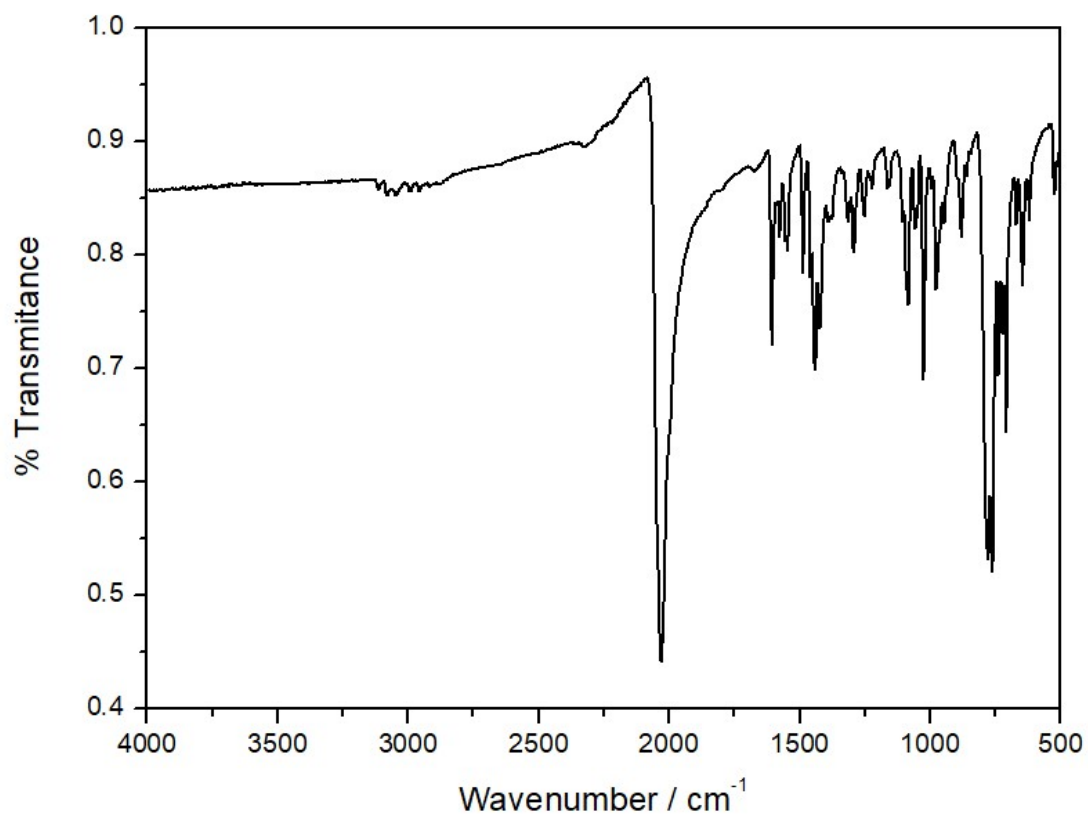


Figure S16: IR spectrum of [Fe^{II}(L^{TetraPy-ODA})(NCS)₂] (C1).

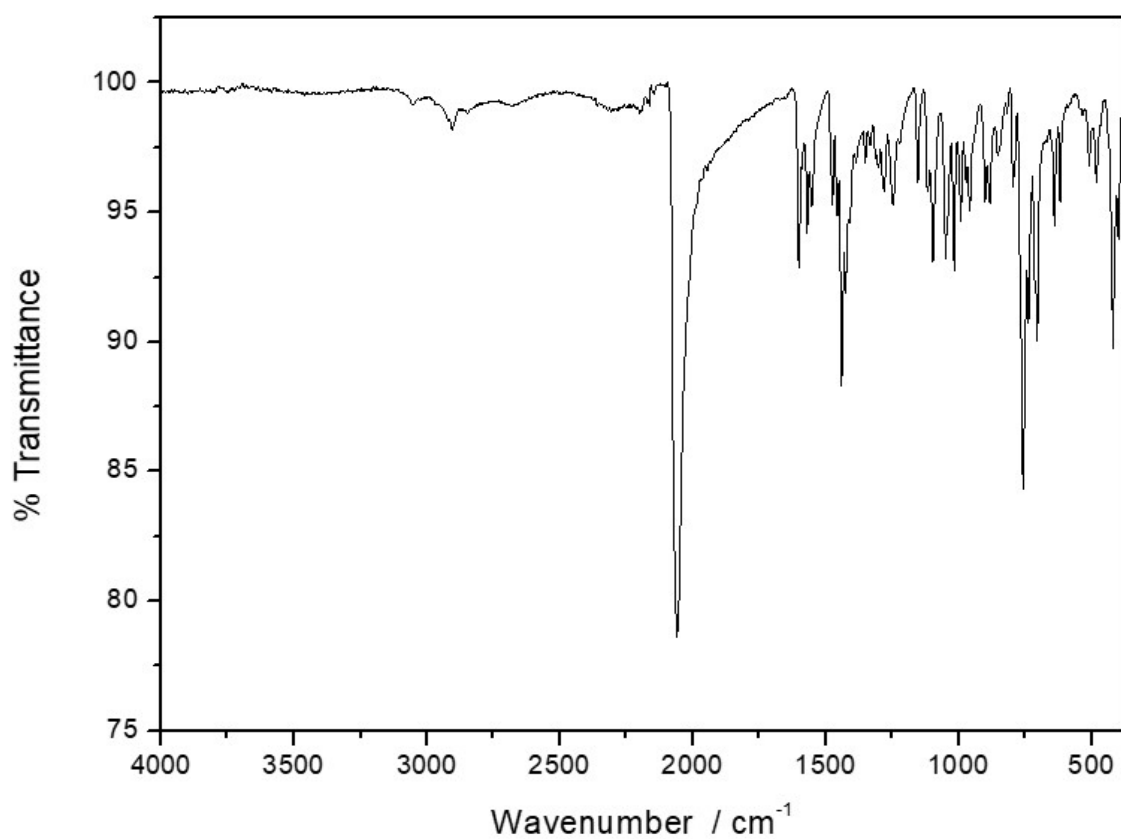


Figure S17: IR spectrum of $[\text{Fe}^{\text{II}}(\text{L}^{\text{TetraPy-ODA}})(\text{NCBSe})_2]$ (C2).

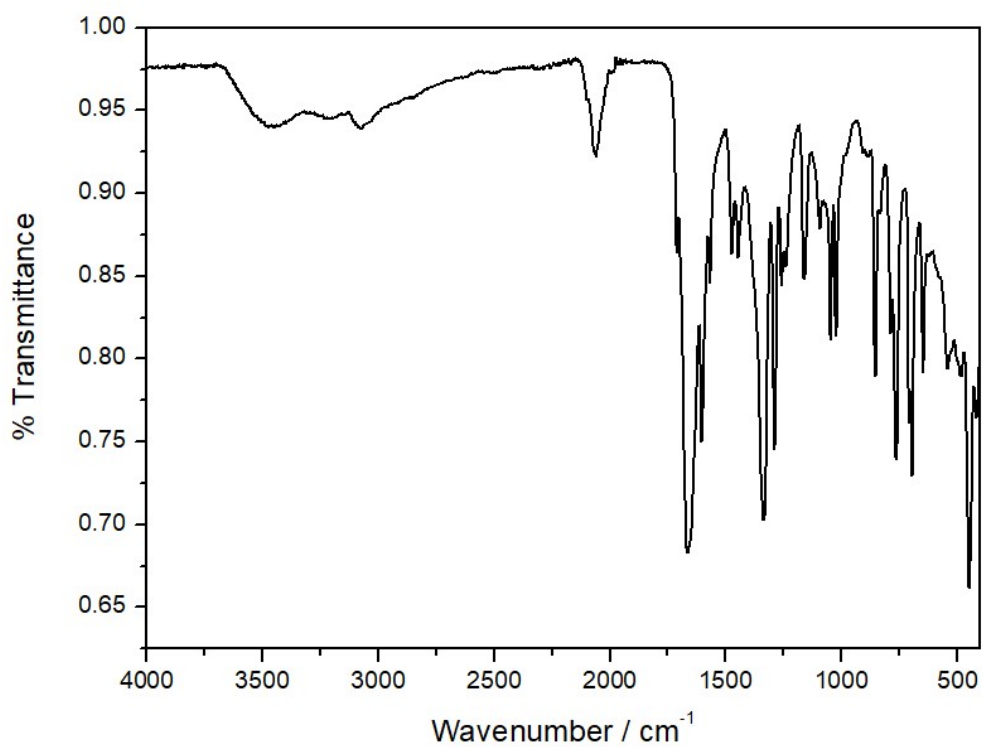


Figure S18: IR spectrum of $[\text{Fe}^{\text{II}}(\text{L}^{\text{TetraPy-ODA}})(\text{NCBH}_3)_2]$ (C3).

3. Crystal data:

Table S1: X-ray crystallographic data for complex **C1** and **C2**

Compound	C1	C2
Empirical formula	C ₂₄ H ₂₁ FeN ₉ OS ₂	C ₂₈ H ₂₇ FeN ₁₁ OSe ₂
Formula weight / g mol ⁻¹	571.47	747.37
Crystal size / mm	0.15 x 0.093 x 0.06	0.38 x 0.293 x 0.24
Crystal system	monoclinic	monoclinic
Space group	<i>P2₁/c</i>	<i>P2₁/c</i>
Unit cell dimensions		
<i>a</i> / Å	15.4394(3)	16.8096(5)
<i>b</i> / Å	11.5893(2)	12.3242(2)
<i>c</i> / Å	23.9234(4)	17.0638(5)
α / °	90	90
β / °	141.138(2)	112.630(2)
γ / °	90	90
Volume / Å ³	2685.90(11)	3262.85(15)
<i>Z</i>	4	4
$\rho_{\text{calc.}}$ / g cm ⁻³	1.413	1.521
μ / mm ⁻¹	0.752	2.733
<i>F</i> (000)	1176	1496
Temperature / K	120	173
Diffractometer	STOE STADIVARI	STOE STADIVARI
Radiation	Mo-K α	Mo-K α
ϑ – range for data collection / °	2.102 < ϑ < 30.782	2.098 < ϑ < 31.109
Index ranges	-21 < <i>h</i> < 22 -16 < <i>k</i> < 16 -34 < <i>l</i> < 31	-24 < <i>h</i> < 24 -17 < <i>k</i> < 17 -20 < <i>l</i> < 23
Collected reflections	48282	60603
Independent reflections	7725	61872
Completeness	0.919	0.907
Max. and min. transmission	0.9853 and 0.6395	0.8343 and 0.3674
<i>R</i> _{int}	0.0221	0.0422
<i>R</i> _{sigma}	0.0181	0.0381
Data/ restraints/ parameters	7725 / 0 / 335	9526 / 0 / 391
Goodness-of-fit on <i>F</i> ²	1.053	0.946
Final <i>R</i> ₁ [<i>I</i> ≥ 2σ(<i>I</i>)]	0.0259	0.0293
Final <i>wR</i> ₂ [<i>I</i> ≥ 2σ(<i>I</i>)]	0.0708	0.0645
Final <i>R</i> ₁ [<i>alldata</i>]	0.0336	0.0529
Final <i>wR</i> ₂ [<i>alldata</i>]	0.0730	0.0688

Table S2: X-ray crystallographic data for complex **C3**. The crystallographic data collected was refined as a twin.

Compound	C3
Empirical formula	C ₂₄ H ₂₇ B ₂ FeN ₉ O
Formula weight / g mol ⁻¹	535.01
Crystal size / mm	0.13 x 0.097 x 0.08
Crystal system	monoclinic
Space group	C2/c
Unit cell dimensions	
a / Å	24.0862 (11)
b / Å	10.9735 (4)
c / Å	20.5959 (8)
α / °	90
β / °	91.577 (3)
γ / °	90
Volume / Å ³	5441.6 (4)
Z	8
ρ _{calc.} / g cm ⁻³	1.306
μ / mm ⁻¹	0.589
F(000)	2224
Temperature / K	173
Diffractometer	STOE STADIVARI
Radiation	Mo-Kα
θ – range for data collection / °	
Index ranges	-34 < h < 34 -15 < k < 15 -29 < l < 29
Collected reflections	51502
Independent reflections	51502
Completeness	
Max. and min. transmission	
R _{int}	
R _{sigma}	0.0360
Data/ restraints/ parameters	51502/0/338
Goodness-of-fit on F ²	1.036
Final R ₁ [I ≥ 2σ(I)]	0.0626
Final wR ₂ [I ≥ 2σ(I)]	0.1668
Final R ₁ [all data]	0.0916
Final wR ₂ [all data]	0.1924

Table S3: X-ray crystallographic data for complex **C4** and **C5**

Compound	C4	C5
Empirical formula	C ₂₇ H ₂₅ FeN ₉ OS ₂	C ₂₈ H _{26.5} FeN _{9.5} OSe ₂
Formula weight / g mol ⁻¹	611.53	725.86
Crystal size / mm	0.32 x 0.207 x 0.11	1.1 x 0.73 x 0.29
Crystal system	monoclinic	monoclinic
Space group	C2/c	C2/c
Unit cell dimensions		
a / Å	30.6059(10)	30.7836(16)
b / Å	11.7584(5)	11.8309(4)
c / Å	17.6574(6)	17.8246(10)
α / °	90	90
β / °	105.110(3)	105.213(4)
γ / °	90	90
Volume / Å ³	6134.8(4)	6264.2(5)
Z	8	8
ρ _{calc.} / g cm ⁻³	1.324	1.539
μ / mm ⁻¹	0.664	2.844
F(000)	2528	2904
Temperature / K	173	173
Diffractometer	STOE STADIVARI	STOE STADIVARI
Radiation	Mo-Kα	Mo-Kα
ϑ – range for data collection / °	1.864 < ϑ < 30.969	1.853 < ϑ < 25.998
Index ranges	-38 < h < 43 -16 < k < 16 -25 < l < 25	-37 < h < 37 -14 < k < 14 -21 < l < 21
Collected reflections	56051	42183
Independent reflections	8963	6163
Completeness	0.919	1.000
Max. and min. transmission	0.9852 and 0.2527	0.8170 and 0.1557
R _{int}	0.0282	0.0989
R _{sigma}	0.0266	0.0579
Data/ restraints/ parameters	8963 / 18 / 414	6163 / 36 / 387
Goodness-of-fit on F ²	1.028	0.969
Final R ₁ [I ≥ 2σ(I)]	0.0302	0.0644
Final wR ₂ [I ≥ 2σ(I)]	0.0820	0.1627
Final R ₁ [all data]	0.0415	0.0813
Final wR ₂ [all data]	0.0848	0.1712

Table S4: X-ray crystallographic data for complex **C6**

Compound	C6 at 120 K	C6 at 240 K
Empirical formula	C ₂₅ H ₂₈ B ₂ FeN ₈ O	C ₂₅ H ₂₈ B ₂ FeN ₈ O
Formula weight / g mol ⁻¹	534.02	534.02
Crystal size / mm	0.7 x 0.5 x 0.2	0.7 x 0.5 x 0.2
Crystal system	monoclinic	monoclinic
Space group	C2/c	C2/c
Unit cell dimensions		
a / Å	22.9994(7)	23.819(2)
b / Å	10.7119(2)	11.1057(7)
c / Å	20.7583(6)	20.7090(17)
α / °	90	90
β / °	91.282(2)	91.611(7)
γ / °	90	90
Volume / Å ³	5112.9(2)	5476.0(7)
Z	8	8
ρ _{calc.} / g cm ⁻³	1.387	1.295
μ / mm ⁻¹	0.625	0.584
F(000)	2224	2224
Temperature / K	120	240
Diffractometer	STOE STADIVARI	STOE STADIVARI
Radiation	Mo-Kα	Mo-Kα
ϑ – range for data collection / °	1.963 < ϑ < 30.816	1.968 < ϑ < 30.718
Index ranges	-32 < h < 32 -15 < k < 14 -29 < l < 28	-33 < h < 34 -15 < k < 15 -29 < l < 28
Collected reflections	38963	45829
Independent reflections	40193	47171
Completeness	0.915	0.927
Max. and min. transmission	0.9675 and 0.2137	0.9107 and 0.1064
R _{int}	0.0386	0.0391
R _{sigma}	0.0254	0.0292
Data/ restraints/ parameters	7340 / 0 / 337	7890 / 99 / 366
Goodness-of-fit on F ²	1.076	1.080
Final R ₁ [I ≥ 2σ(I)]	0.0436	0.0387
Final wR ₂ [I ≥ 2σ(I)]	0.1185	0.1116
Final R ₁ [all data]	0.0509	0.0580
Final wR ₂ [all data]	0.1236	0.1185

Table S5: X-ray crystallographic data for complex **C7**

Compound	C7
Empirical formula	C ₄₂ H ₄₂ Cl ₄ Fe ₂ N ₁₄ O ₂₂
Formula weight / g mol ⁻¹	1348.39
Crystal size / mm	0.2 x 0.147 x 0.08
Crystal system	monoclinic
Space group	<i>P</i> 2 ₁ / <i>n</i>
Unit cell dimensions	
<i>a</i> / Å	12.5361(4)
<i>b</i> / Å	16.0432(6)
<i>c</i> / Å	13.6085(5)
α / °	90
β / °	95.600(3)
γ / °	90
Volume / Å ³	2723.87(17)
<i>Z</i>	2
$\rho_{\text{calc.}}$ / g cm ⁻³	1.644
μ / mm ⁻¹	0.822
F(000)	1376
Temperature / K	150(2)
Diffractometer	STOE STADIVARI
Radiation	Mo-K α
ϑ – range for data collection / °	1.968 < ϑ < 30.803
Index ranges	-16 < <i>h</i> < 17 -21 < <i>k</i> < 22 -19 < <i>l</i> < 19
Collected reflections	31060
Independent reflections	7639
Completeness	0.895
Max. and min. transmission	0.6837 and 0.5083
<i>R</i> _{int}	0.0246
<i>R</i> _{sigma}	0.0307
Data/ restraints/ parameters	7639 / 18 / 445
Goodness-of-fit on <i>F</i> ²	1.036
Final <i>R</i> ₁ [<i>I</i> ≥ 2σ(<i>I</i>)]	0.0328
Final <i>wR</i> ₂ [<i>I</i> ≥ 2σ(<i>I</i>)]	0.0793
Final <i>R</i> ₁ [<i>all</i> data]	0.0509
Final <i>wR</i> ₂ [<i>all</i> data]	0.0842

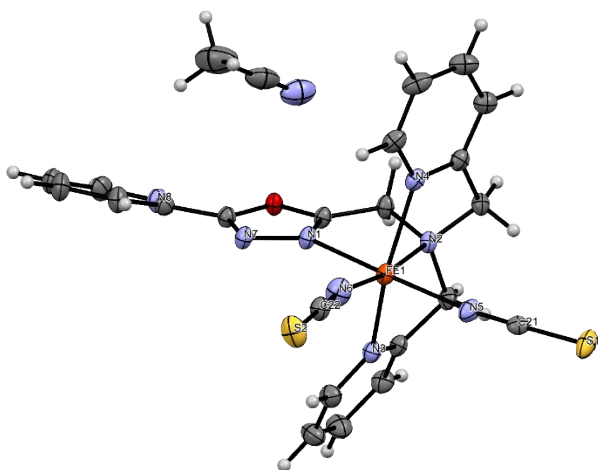


Figure S19: Asymmetric Unit of $[\text{Fe}_2^{\text{II}}(\text{L}^{\text{TetraPy-ODA}})(\text{NCS})] \cdot \text{H}_2\text{O}$ (**C1**). ORTEP representation with atomic displacement parameters set to 50 % probability.

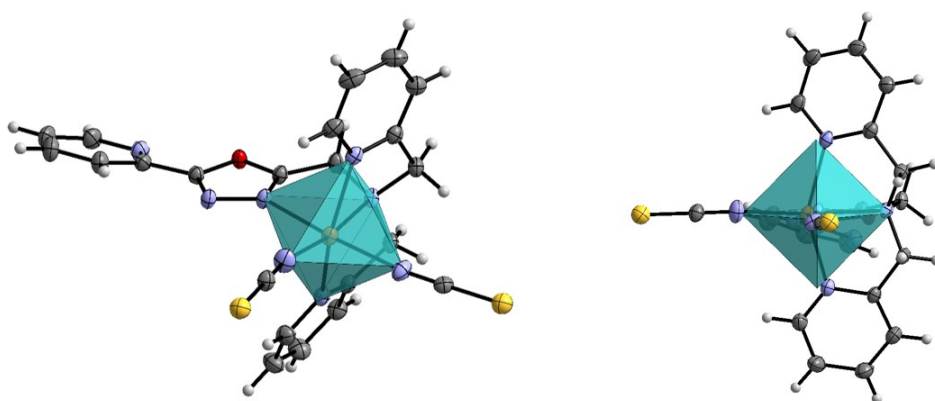


Figure S20: Molecular structure of $[\text{Fe}_2^{\text{II}}(\text{L}^{\text{TetraPy-ODA}})(\text{NCS})] \cdot \text{H}_2\text{O}$ (**C1**) and its ideal coordination octahedron with front view (left) and view along the Fe-N5 axis (right), calculated with SHAPE.¹ Colour scheme: dark grey – C, grey – H, violet – N, red – O, yellow – S, orange – Fe. ORTEP representation with atomic displacement parameters set to 50 % probability.

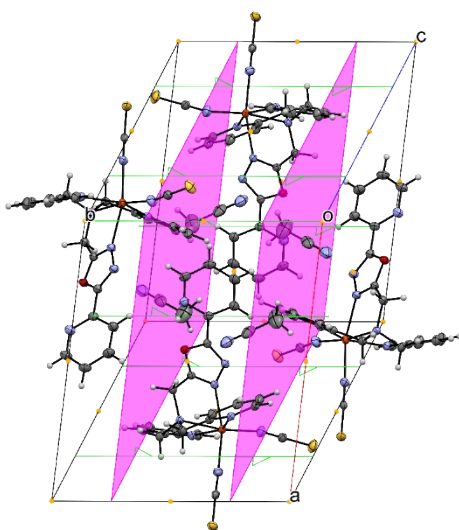


Figure S21: Perspective view onto the unit cell of $[\text{Fe}_2^{\text{II}}(\text{L}^{\text{TetraPy-ODA}})(\text{NCS})] \cdot \text{H}_2\text{O}$ (**C1**) with present symmetry elements. Centers of Inversion – yellow dots, Two-fold Axis – green lines, Mirror Glide Plane – purple planes.

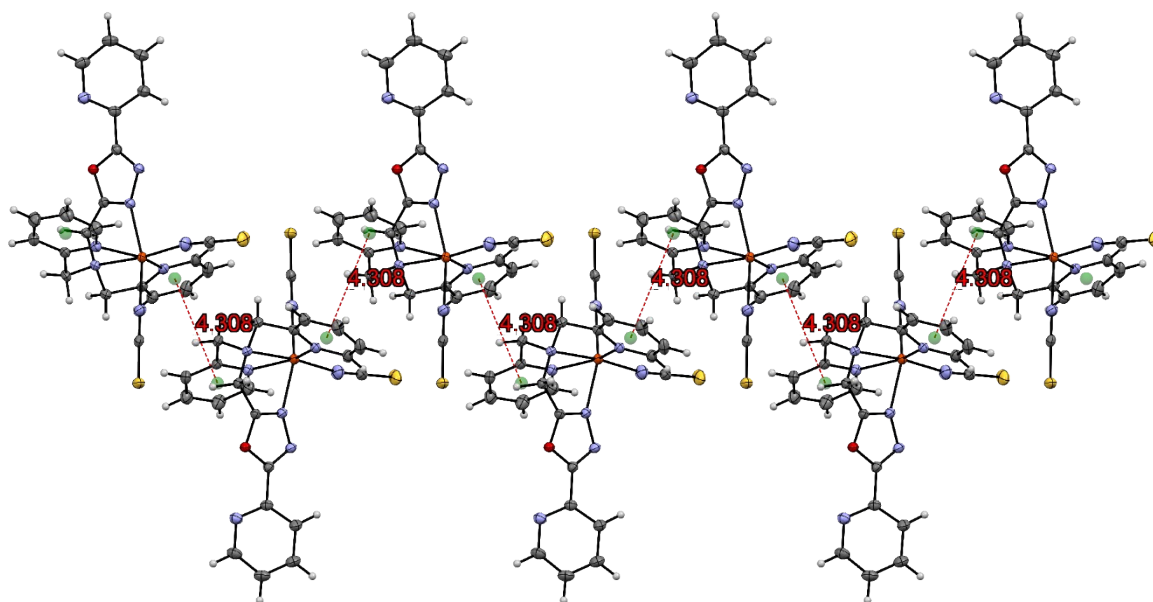


Figure S22: One dimensional chain formed by π - π interactions in $[\text{Fe}_2^{\text{II}}(\text{L}^{\text{TetraPy-ODA}})(\text{NCS})] \cdot \text{H}_2\text{O}$ (**C1**). Green points – centres of aromatic rings involved in π - π interactions. Red dashed lines – centre-to-centre distance. Distances between the centres of two interacting aromatic rings are displayed in red. ORTEP representation with atomic displacement parameters set to 50 % probability.

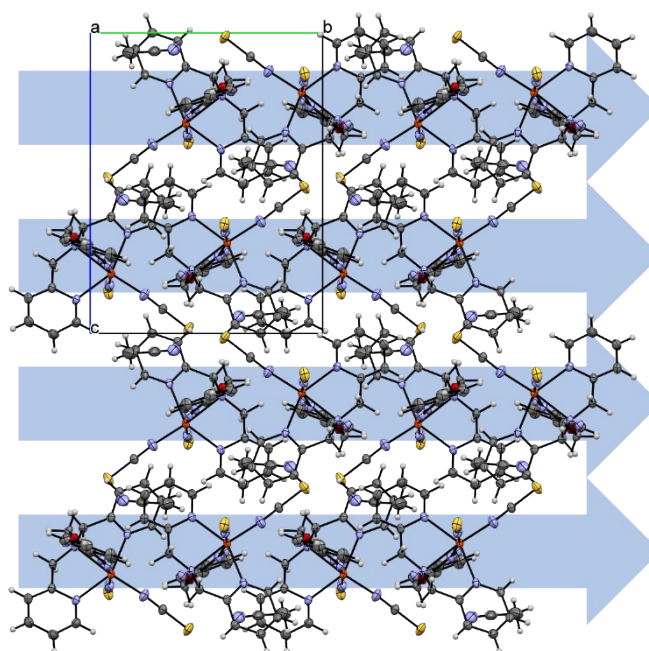


Figure S23: One dimensional chain formed by π - π interactions in the packing of $[\text{Fe}_2^{\text{II}}(\text{L}^{\text{TetraPy-ODA}})(\text{NCS})] \cdot \text{H}_2\text{O}$ (**C1**) with view along the a-axis. Blue arrows indicate the chains along the b-axis. ORTEP representation with atomic displacement parameters set to 50 % probability.

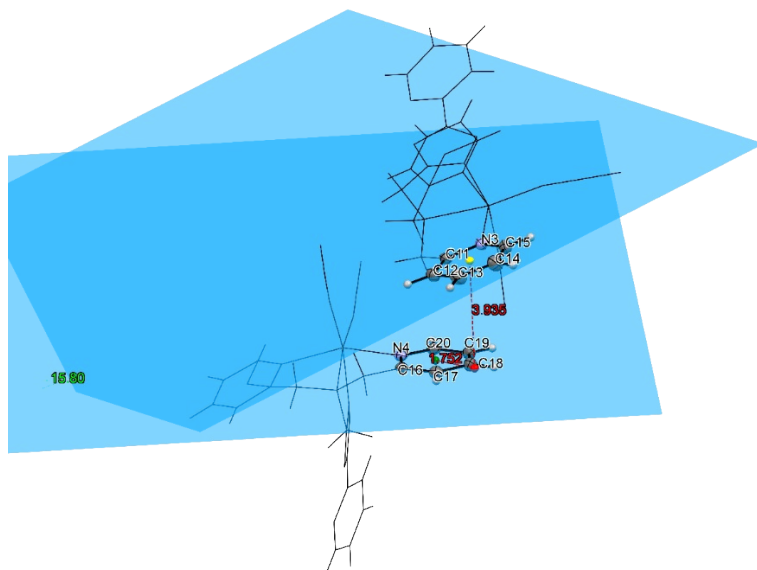


Figure S24: π - π interaction in $[\text{Fe}_2^{\text{II}}(\text{L}^{\text{TetraPy-ODA}})(\text{NCS})] \cdot \text{H}_2\text{O}$ (**C1**). Least-squares mean plane A is defined by N4, C16, C17, C18, C19 and C20. Plane B is defined by N3, C11, C12, C13, C14 and C15. Green point – centre of the aromatic ring in A. Yellow point – center of the aromatic ring in B. Red point – orthogonal intersection of the aromatic centre in B onto plane A. Offset $r = 1.752\text{\AA}$, interplanar distance $d_{\text{AB}} = 3.959\text{\AA}$, interplanar angle $\theta = 15.80^\circ$. ORTEP representation with atomic displacement parameters set to 50 % probability.

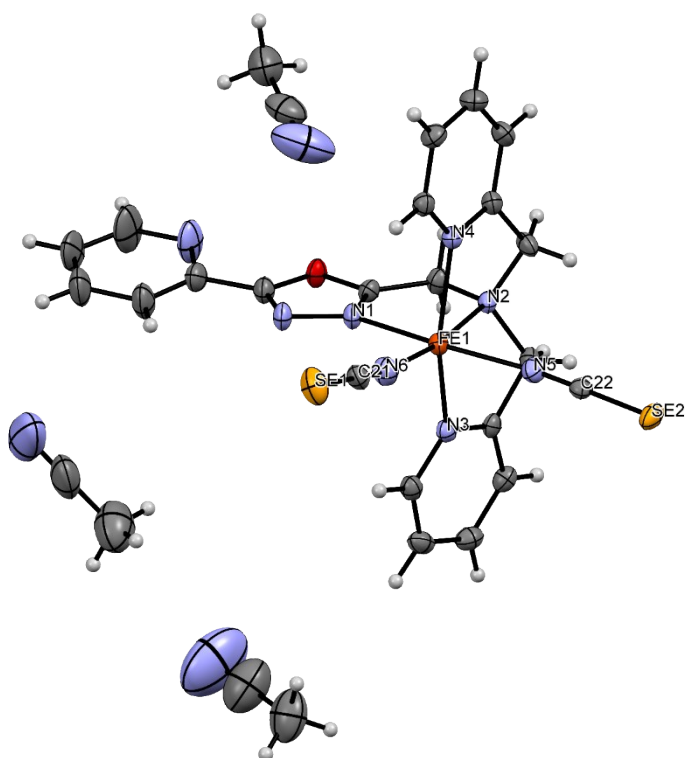


Figure S25: Asymmetric Unit of $[\text{Fe}_2^{\text{II}}(\text{L}^{\text{TetraPy-ODA}})(\text{NCSe})] \cdot 0.15 \text{CH}_3\text{CN} \cdot 1.5 \text{H}_2\text{O}$ (**C2**). ORTEP representation with atomic displacement parameters set to 50 % probability.

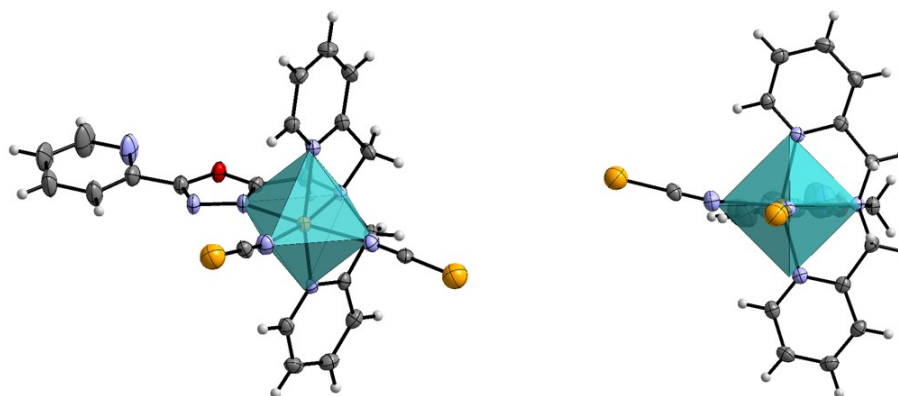


Figure S26: Molecular structure of $[\text{Fe}_2^{\text{II}}(\text{L}^{\text{TetraPy-ODA}})(\text{NCSe})] \cdot 0.15 \text{ CH}_3\text{CN} \cdot 1.5 \text{ H}_2\text{O}$ (**C2**) and its ideal coordination octahedron with front view (left) and view along the Fe-N5 axis (right), calculated with SHAPE.¹ Colour scheme: dark grey – C, grey – H, violet – N, red – O, bright orange – Se, orange – Fe. ORTEP representation with atomic displacement parameters set to 50 % probability.

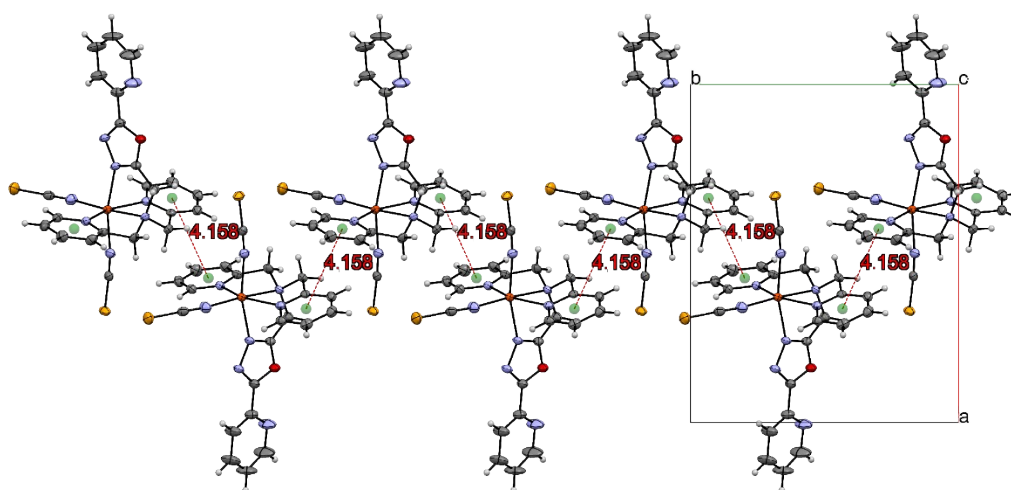


Figure S27: One-dimensional chain of complex molecules in $[\text{Fe}_2^{\text{II}}(\text{L}^{\text{TetraPy-ODA}})(\text{NCSe})] \cdot 0.15 \text{ CH}_3\text{CN} \cdot 1.5 \text{ H}_2\text{O}$ (**C2**) due to intermolecular π - π stacking along the b-axis. The centres of involved aromatic rings are displayed as green points. Red dashed lines and numbers represent the distance between two centres.

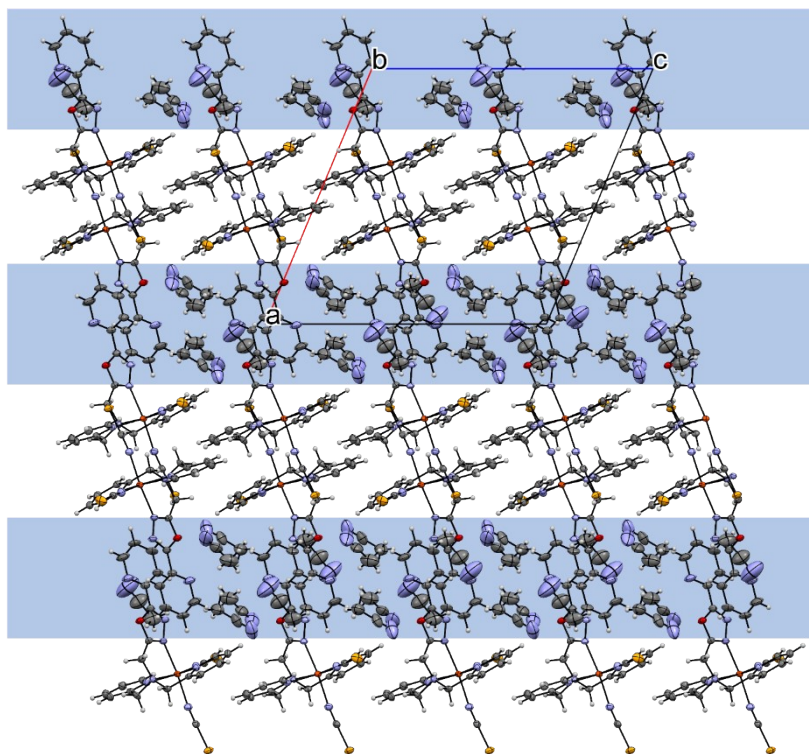


Figure S28: Packing of $[\text{Fe}_2^{\text{II}}(\text{L}^{\text{TetraPy-ODA}})(\text{NCSe})] \cdot 0.15 \text{ CH}_3\text{CN} \cdot 1.5 \text{ H}_2\text{O}$ (**C2**) with view along the b-axis. Blue areas illustrate the layers of solvent molecules. ORTEP representation with atomic displacement parameters set to 50 % probability.

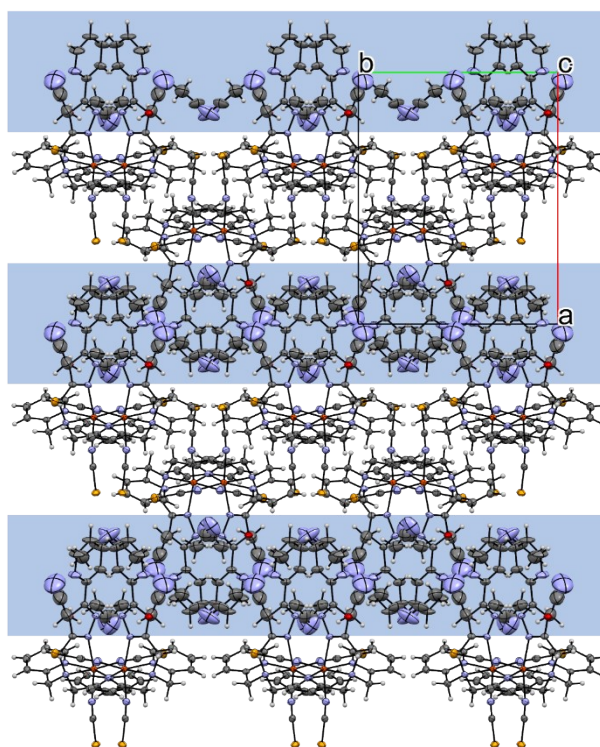


Figure S29: Packing of $[\text{Fe}_2^{\text{II}}(\text{L}^{\text{TetraPy-ODA}})(\text{NCSe})] \cdot 0.15 \text{ CH}_3\text{CN} \cdot 1.5 \text{ H}_2\text{O}$ (**C2**) with view along the c-axis. Blue areas illustrate the layers of solvent molecules. ORTEP representation with atomic displacement parameters set to 50 % probability.

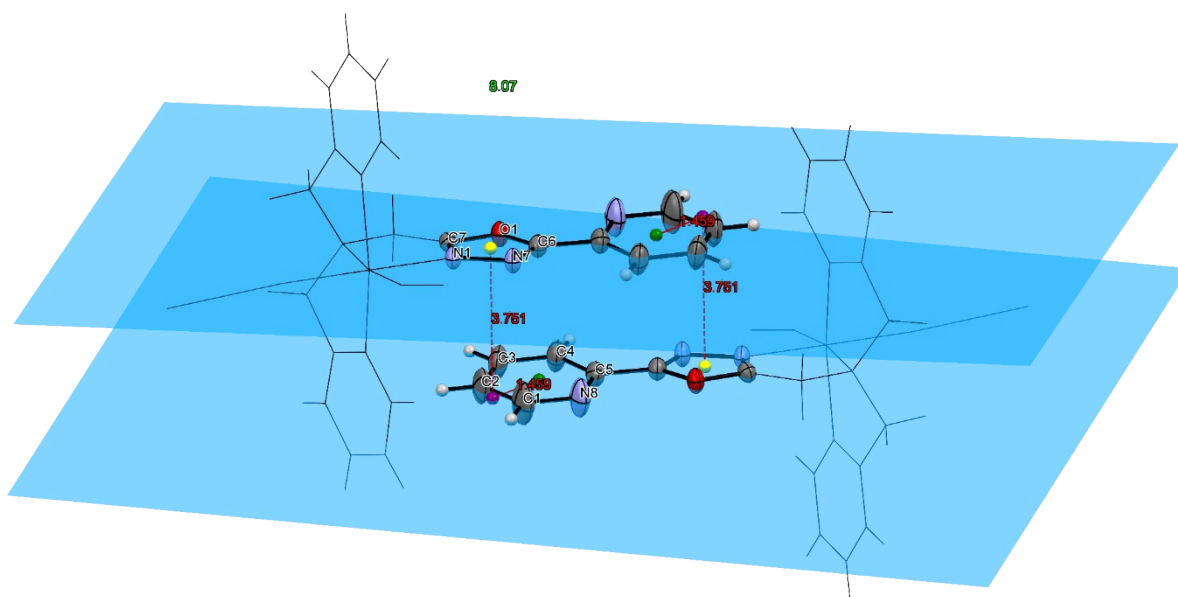


Figure S30: π - π interaction in $[\text{Fe}_2^{\text{II}}(\text{L}^{\text{TetraPy-ODA}})(\text{NCSe})] \cdot 0.15 \text{ CH}_3\text{CN} \cdot 1.5 \text{ H}_2\text{O}$ (**C2**). Least-squares mean plane A is defined by N8, C1, C2, C3, C4 and C5. Plane B is defined by O1, C6, N7, N1 and C7 of an adjacent molecule. Green point – centre of the aromatic ring in A. Yellow point – centre of the aromatic ring in B. Purple point – orthogonal intersection of the aromatic center in B onto plane A. Offset $r = 1.459 \text{ \AA}$, interplanar distance $d_{\text{AB}} = 3.751 \text{ \AA}$, interplanar angle $\vartheta = 8.07^\circ$. ORTEP representation with atomic displacement parameters set to 50 % probability.

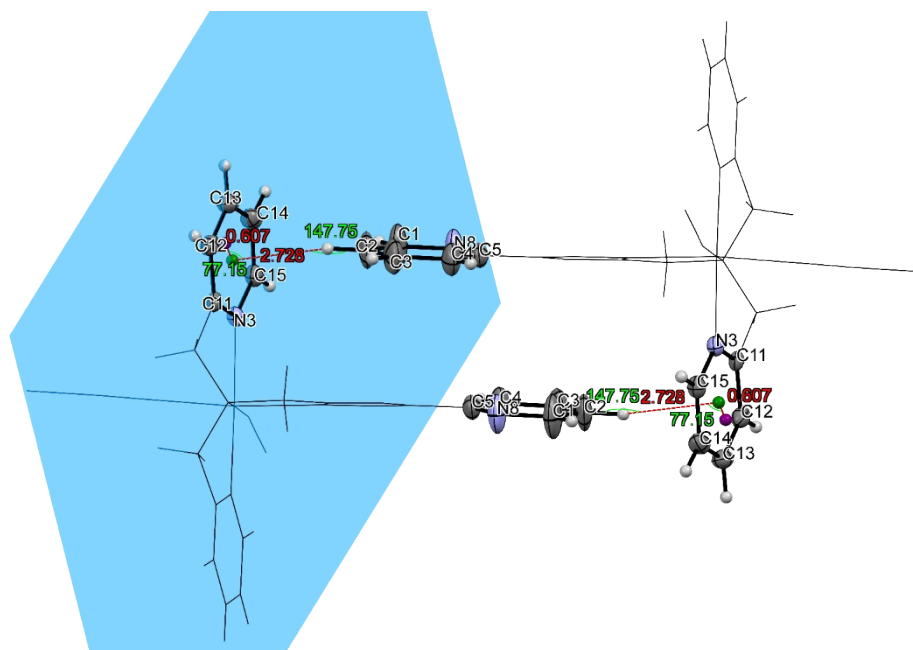


Figure S31: C-H... π interaction in $[\text{Fe}_2^{\text{II}}(\text{L}^{\text{TetraPy-ODA}})(\text{NCSe})] \cdot 0.15 \text{ CH}_3\text{CN} \cdot 1.5 \text{ H}_2\text{O}$ (**C2**). Least-squares plane A is defined by N3, C11, C12, C13, C14 and C15. Interacting C-H fragment is labelled as C2-H2. Green point – centre of the aromatic ring in A. Purple point – orthogonal intersection of H2 onto plane A. Offset $r = 0.607 \text{ \AA}$, interaction distance $d_{\text{QH}} = 2.728 \text{ \AA}$, $\alpha = 147.75^\circ$ and $\beta = 77.15^\circ$. ORTEP representation with atomic displacement parameters set to 50 % probability.

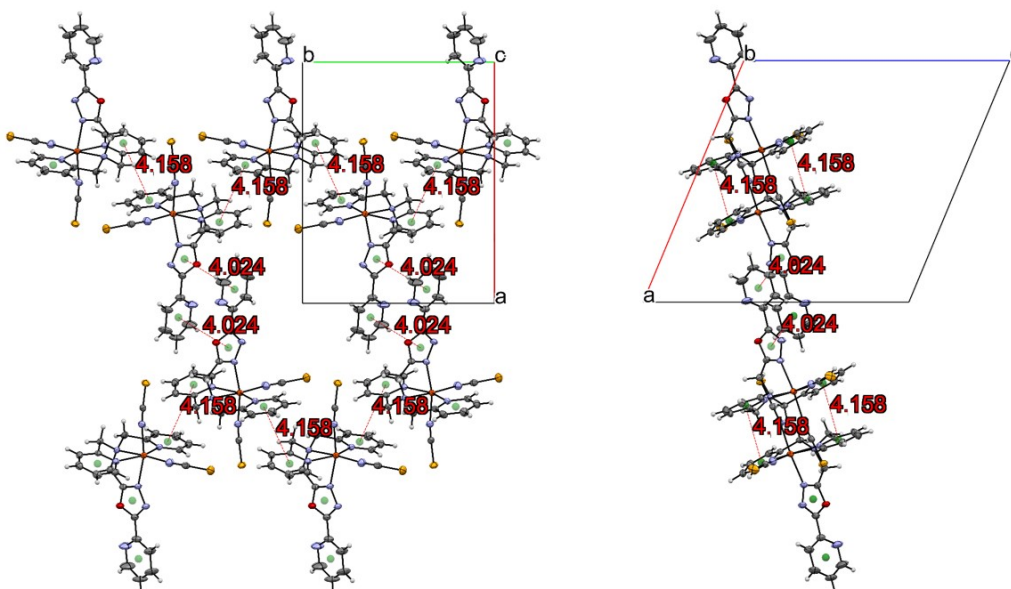


Figure S32: Two-dimensional network of complex molecules in $[\text{Fe}_2^{\text{II}}(\text{L}^{\text{TetraPy-ODA}})(\text{NCSe})] \cdot 0.15 \text{CH}_3\text{CN} \cdot 1.5 \text{H}_2\text{O}$ (**C2**), due to intermolecular π - π interactions with view along the c-axis (left) and b-axis (right). The centres of involved aromatic rings are displayed as green points. Distances are displayed as red dashed lines and numbers. Solvent molecules are omitted for better vision.

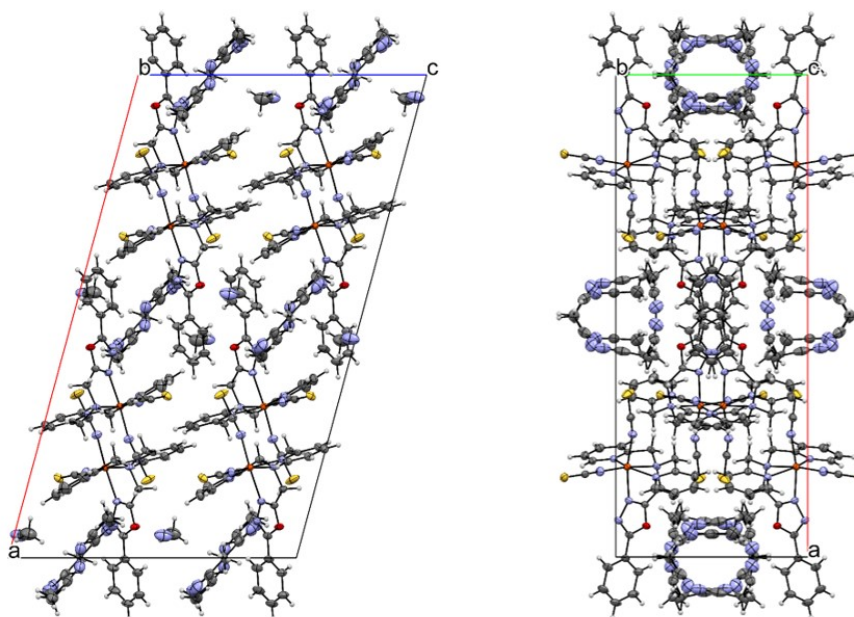


Figure S33: Left: Unit cell of $[\text{Fe}_2^{\text{II}}(\text{L}^{\text{TetraPh-ODA}})(\text{NCS})] \cdot 1.75 \text{H}_2\text{O}$ (**C4**) with view along the b-axis. Right: Unit cell of $[\text{Fe}_2^{\text{II}}(\text{L}^{\text{TetraPh-ODA}})(\text{NCS})] \cdot 1.75 \text{H}_2\text{O}$ (**C4**) with view along the c-axis. ORTEP representation with atomic displacement parameters set to 50 % probability.

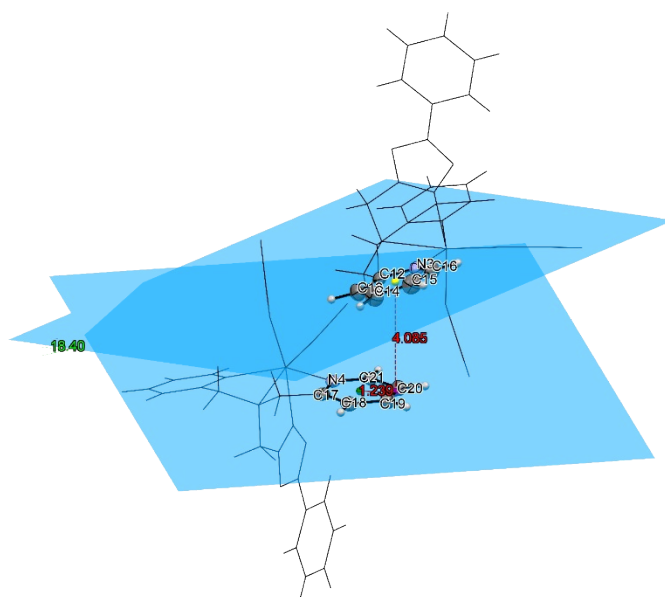


Figure S34: π - π interaction in $[\text{Fe}_2^{\text{II}}(\text{L}^{\text{TetraPh-ODA}})(\text{NCS})] \cdot 1.75 \text{ H}_2\text{O}$ (**C4**). Least-squares mean plane A is defined by N4, C17, C18, C19, C20 and C21. Plane B is defined by N3, C12, C13, C14, C15 and C16 of an adjacent molecule. Green point – centre of the aromatic ring in A. Yellow point – centre of the aromatic ring in B. Purple point – orthogonal intersection of the aromatic centre in B onto plane A. Offset $r = 1.239 \text{ \AA}$, interplanar distance $d_{\text{AB}} = 4.085 \text{ \AA}$, interplanar angle $\theta = 18.40^\circ$. ORTEP representation with atomic displacement parameters set to 50 % probability.

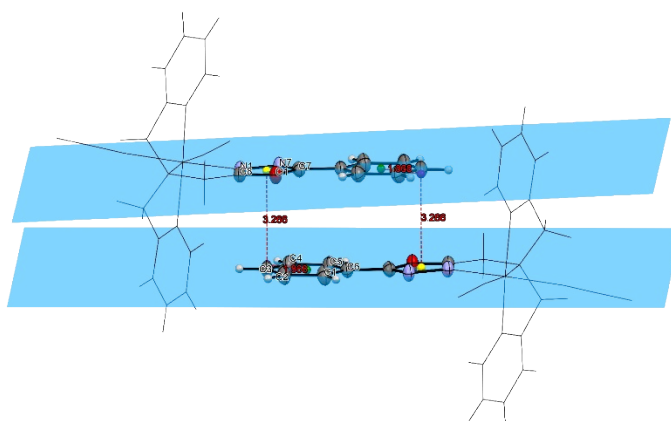


Figure S35: π - π interaction in $[\text{Fe}_2^{\text{II}}(\text{L}^{\text{TetraPh-ODA}})(\text{NCS})] \cdot 1.75 \text{ H}_2\text{O}$ (**C4**). Least-squares mean plane A is defined by C1, C2, C3, C4, C5 and C6. Plane B is defined by O1, C7, N7, N1 and C8 of an adjacent molecule. Green point – centre of the aromatic ring in A. Yellow point – centre of the aromatic ring in B. Purple point – orthogonal intersection of the aromatic centre in B onto plane A. Offset $r = 1.868 \text{ \AA}$, interplanar distance $d_{\text{AB}} = 3.266 \text{ \AA}$, interplanar angle $\theta = 2.7^\circ$. ORTEP representation with atomic displacement parameters set to 50 % probability.

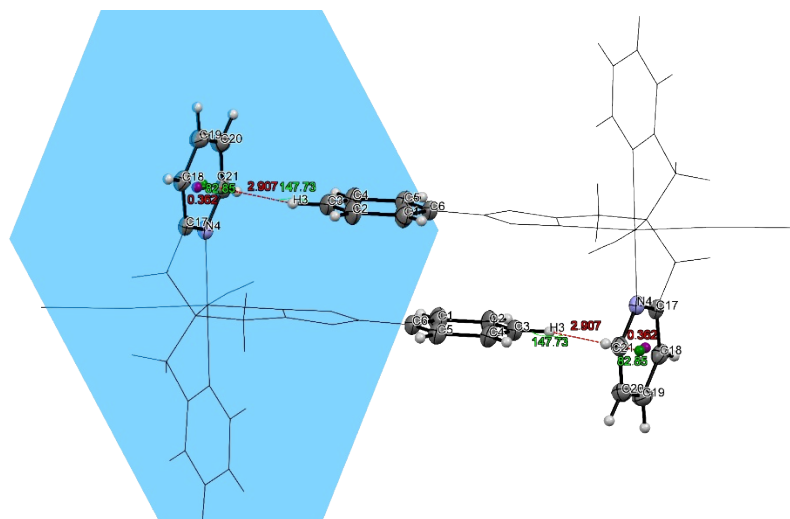


Figure S36: C-H ... π interaction in $[\text{Fe}_2^{\text{II}}(\text{L}^{\text{TetraPh-ODA}})(\text{NCS})] \cdot 1.75 \text{ H}_2\text{O}$ (**C4**). Least-squares plane A is defined by N4, C17, C18, C19, C20 and C21. Interacting C-H fragment is labeled as C3-H3. Green point – center of the aromatic ring in A. Purple point – orthogonal intersection of H13 onto plane A. Offset $r = 0.362 \text{ \AA}$, interaction distance $d_{\text{OH}} = 2.907 \text{ \AA}$, $\alpha = 147.73^\circ$ and $\beta = 82.85^\circ$. ORTEP representation with atomic displacement parameters set to 50 % probability.

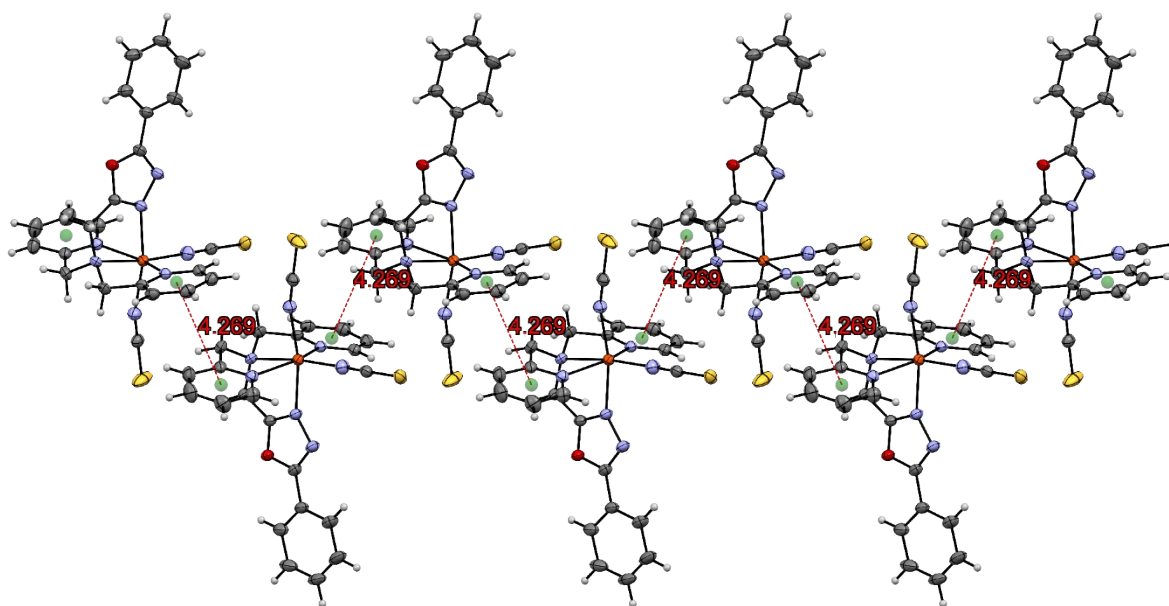


Figure S37: One-dimensional chain of complex molecules in $[\text{Fe}_2^{\text{II}}(\text{L}^{\text{TetraPh-ODA}})(\text{NCS})] \cdot 1.75 \text{ H}_2\text{O}$ (**C4**) due to intermolecular π - π stacking. The centres of involved aromatic rings are displayed as green points. Red dashed lines and numbers represent the distance between two centres. Colour scheme: dark grey – C, grey – H, violet – N, red – O, bright orange – Se, orange – Fe. ORTEP representation with atomic displacement parameters set to 50 % probability.

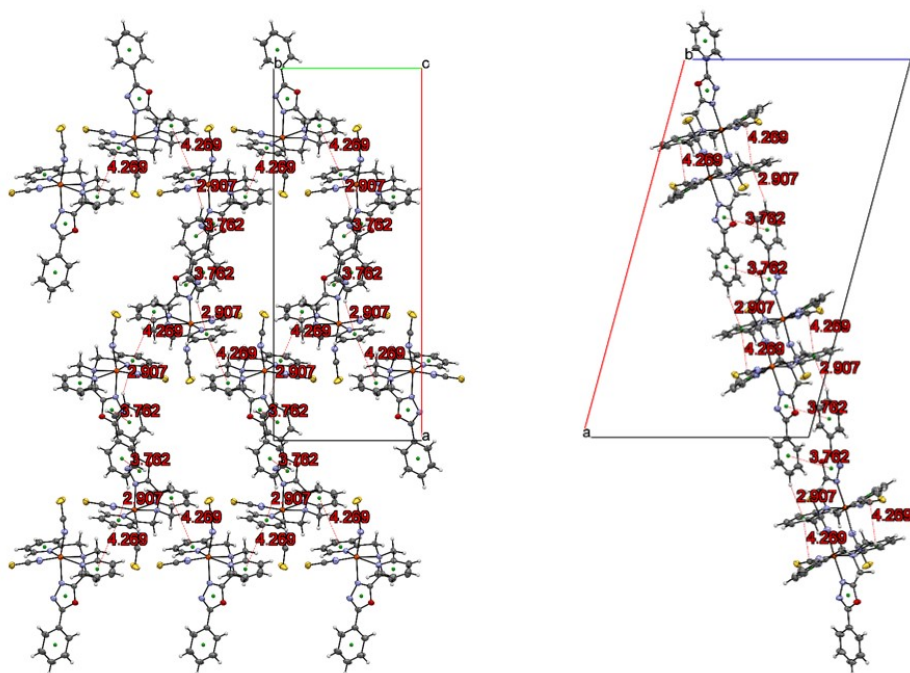


Figure S38: Two-dimensional network of complex molecules in $[\text{Fe}_2^{\text{II}}(\text{L}^{\text{TetraPh-ODA}})(\text{NCS})] \cdot 1.75 \text{H}_2\text{O}$ (**C4**) due to intermolecular π - π interactions with view along the c-axis (left) and b-axis (right). The centres of involved aromatic rings are displayed as green points. Distances are displayed as red dashed lines and numbers. Solvent molecules are omitted for better vision. ORTEP representation with atomic displacement parameters set to 50 % probability.

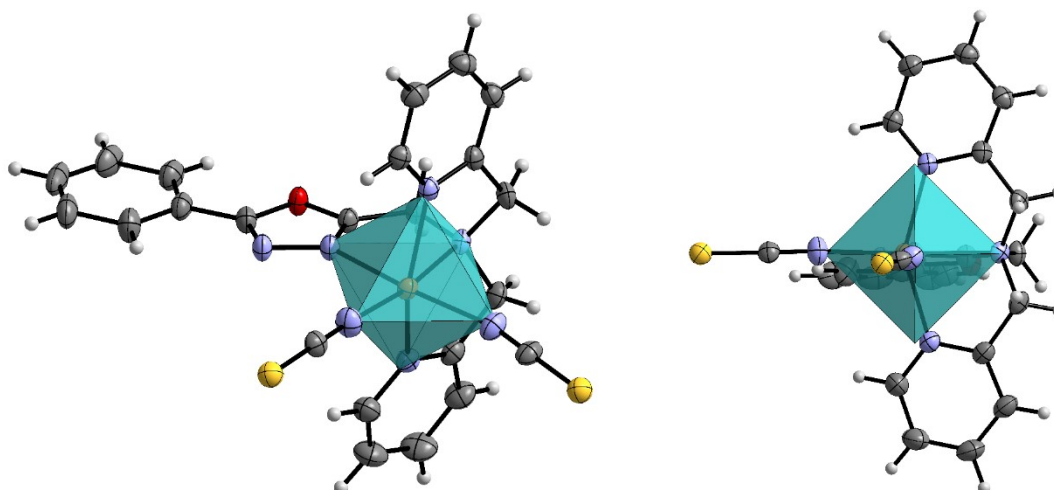


Figure S39: Molecular structure of $[\text{Fe}_2^{\text{II}}(\text{L}^{\text{TetraPh-ODA}})(\text{NCS})] \cdot 1.75 \text{H}_2\text{O}$ (**C4**) and its ideal coordination octahedron with front view (left) and view along the Fe-N5 axis (right), calculated with SHAPE.¹ ORTEP representation with atomic displacement parameters set to 50 % probability.

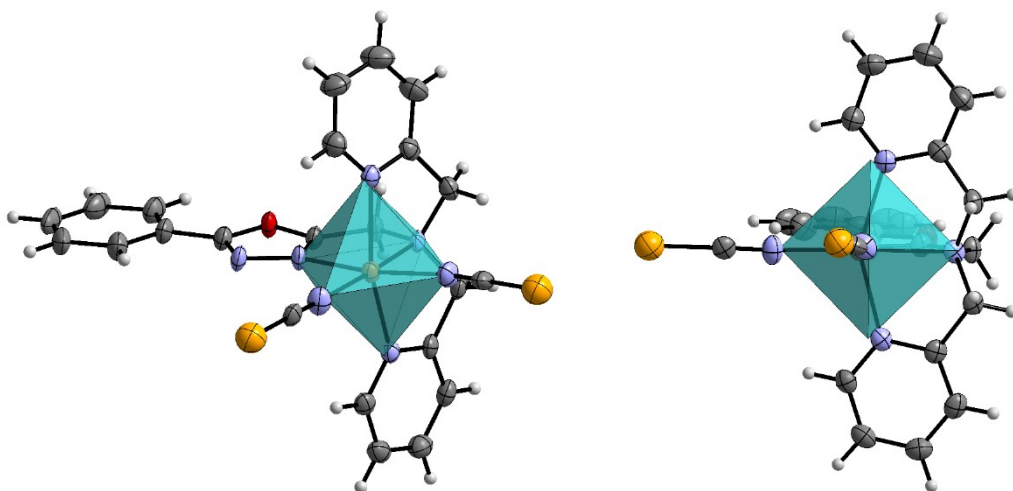


Figure S40: Molecular structure of $[\text{Fe}_2^{\text{II}}(\text{L}^{\text{TetraPh-ODA}})(\text{NCSe})] \cdot 0.4\text{Et}_2\text{O} \cdot \text{H}_2\text{O}$ (**C5**) and its ideal coordination octahedron with front view (left) and view along the Fe-N5 axis (right), calculated with SHAPE.¹ ORTEP representation with atomic displacement parameters set to 50 % probability.

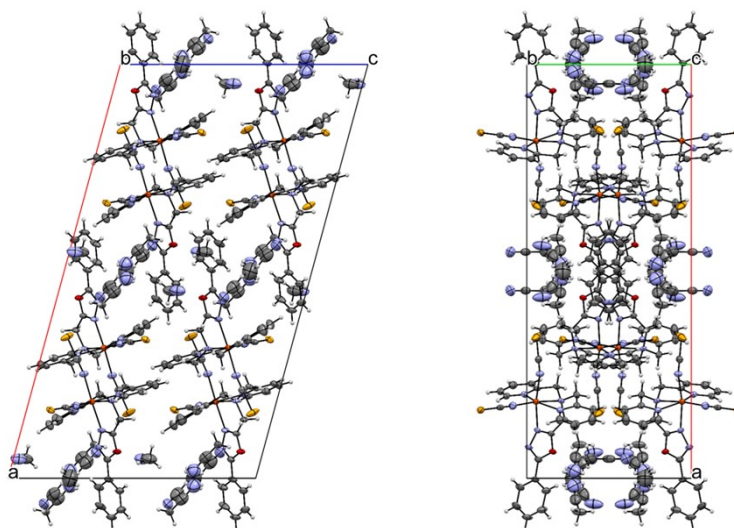


Figure S41: Unit cell of $[\text{Fe}_2^{\text{II}}(\text{L}^{\text{TetraPh-ODA}})(\text{NCSe})] \cdot 0.4\text{Et}_2\text{O} \cdot \text{H}_2\text{O}$ (**C5**) with view along the b-axis (left) and view along the c-axis (right). ORTEP representation with atomic displacement parameters set to 50 % probability.

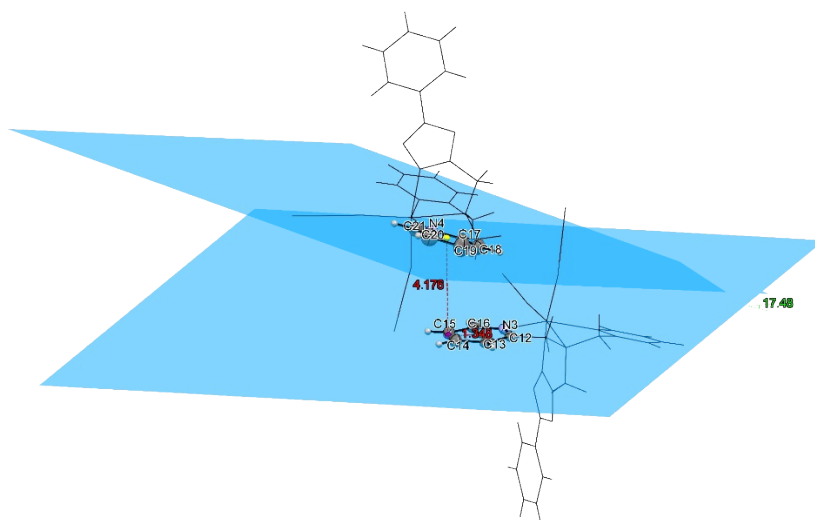


Figure S42: π - π interaction in $[\text{Fe}_2^{\text{II}}(\text{L}^{\text{TetraPh-ODA}})(\text{NCSe})] \cdot 0.4\text{Et}_2\text{O} \cdot \text{H}_2\text{O}$ (**C5**). Least-squares mean plane A is defined by N3, C12, C13, C14, C15 and C16. Plane B is defined by N4, C17, C18, C19, C20 and C21 of an adjacent molecule. Green point – centre of the aromatic ring in A. Yellow point – centre of the aromatic ring in B. Purple point – orthogonal intersection of the aromatic centre in B onto plane A. Offset $r = 1.348 \text{ \AA}$, interplanar distance $d_{\text{AB}} = 4.176 \text{ \AA}$, interplanar angle $\vartheta = 17.48^\circ$. ORTEP representation with atomic displacement parameters set to 50 % probability.

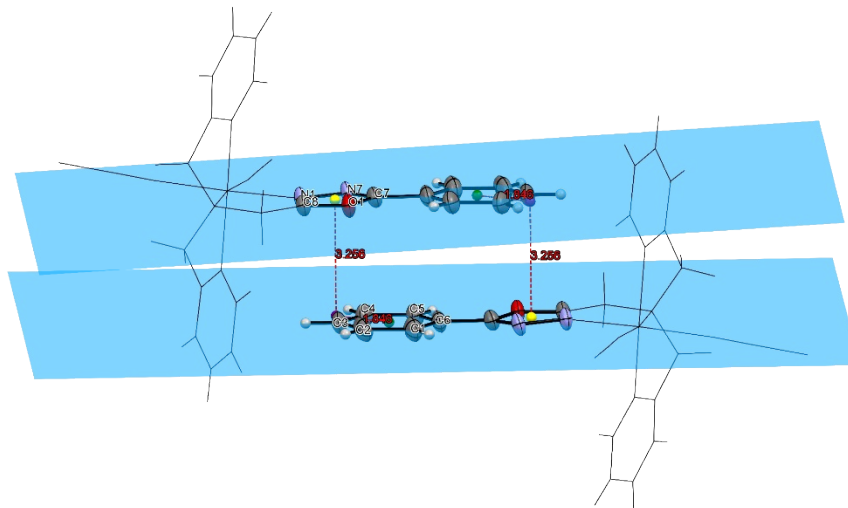


Figure S43: π - π interaction in $[\text{Fe}_2^{\text{II}}(\text{L}^{\text{TetraPh-ODA}})(\text{NCSe})] \cdot 0.4\text{Et}_2\text{O} \cdot \text{H}_2\text{O}$ (**C5**). Least-squares mean plane A is defined by C1, C2, C3, C4, C5 and C6. Plane B is defined by O1, C7, N7, N1 and C8 of an adjacent molecule. Green point – center of the aromatic ring in A. Yellow point – center of the aromatic ring in B. Purple point – orthogonal intersection of the aromatic center in B onto plane A. Offset $r = 1.846 \text{ \AA}$, interplanar distance $d_{\text{AB}} = 3.256 \text{ \AA}$, interplanar angle $\vartheta = 3^\circ$. ORTEP representation with atomic displacement parameters set to 50 % probability.

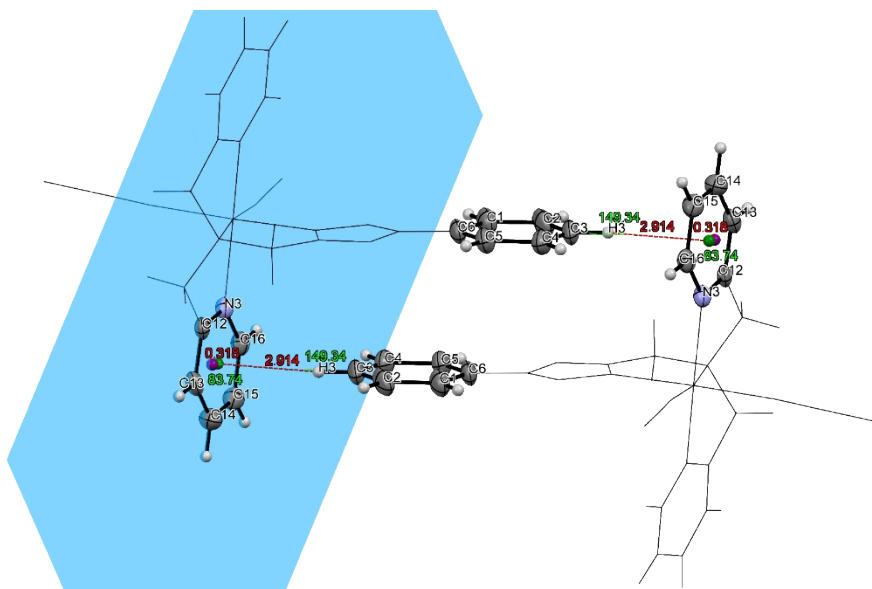


Figure S44: C-H \cdots π interaction in $[\text{Fe}_2^{\text{II}}(\text{L}^{\text{TetraPh-ODA}})(\text{NCSe})] \cdot 0.4\text{Et}_2\text{O} \cdot \text{H}_2\text{O}$ (**C5**). Least-squares plane A is defined by N3, C12, C13, C14, C15 and C16. Interacting C-H fragment is labeled as C3-H3. Green point – center of the aromatic ring in A. Purple point – orthogonal intersection of H13 onto plane A. Offset $r = 0.318 \text{ \AA}$, interaction distance $d_{\text{QH}} = 2.914 \text{ \AA}$, $\alpha = 149.34^\circ$ and $\beta = 83.74^\circ$. ORTEP representation with atomic displacement parameters set to 50 % probability.

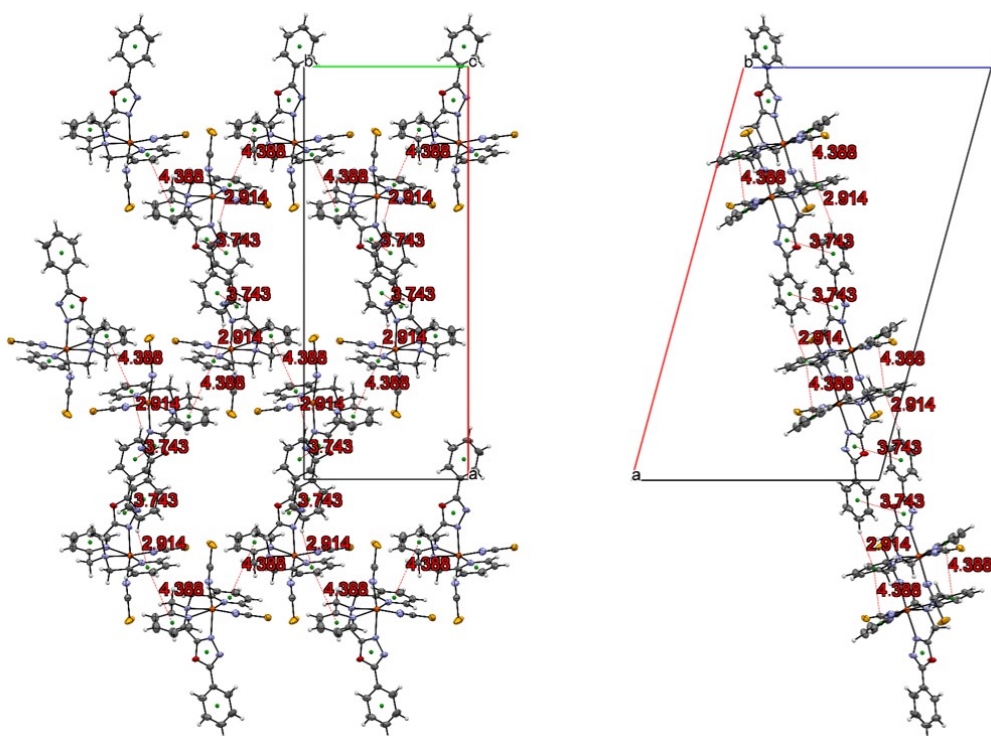


Figure S45: Two-dimensional network of complex molecules in $[\text{Fe}_2^{\text{II}}(\text{L}^{\text{TetraPh-ODA}})(\text{NCSe})] \cdot 0.4\text{Et}_2\text{O} \cdot \text{H}_2\text{O}$ (**C5**) due to intermolecular π - π interactions with view along the c-axis (left) and b-axis (right). The centres of involved aromatic rings are displayed as green points. Distances are displayed as red dashed lines and numbers. Solvent molecules are omitted for better vision. ORTEP representation with atomic displacement parameters set to 50 % probability.

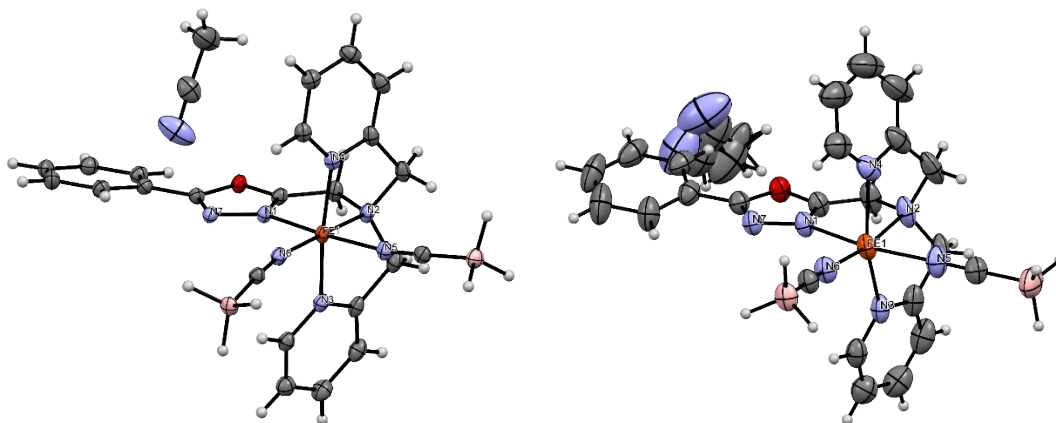


Figure S46: Asymmetric Unit of $[\text{Fe}_2^{\text{II}}(\text{L}^{\text{TetraPh-ODA}})(\text{NCBH}_3)] \cdot 1.5 \text{H}_2\text{O}$ (**C6**) (120 K(left); 240 K (right)). ORTEP representation with atomic displacement parameters set to 50 % probability.

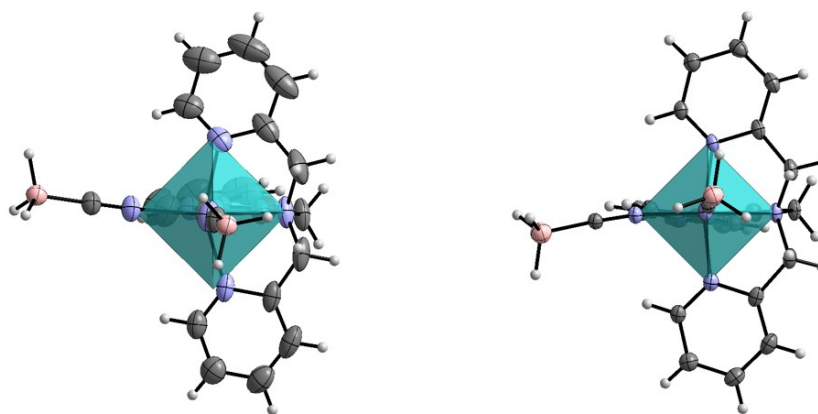


Figure S47: Molecular structure of $[\text{Fe}_2(\text{L}^{\text{TetraPh-ODA}})(\text{NCBH}_3)] \cdot 1.5 \text{H}_2\text{O}$ (C6) and its ideal coordination octahedron with view along the Fe-N5 axis at 240 K (left) and 120 K (right), calculated with SHAPE.¹ ORTEP representation with atomic displacement parameters set to 50 % probability.

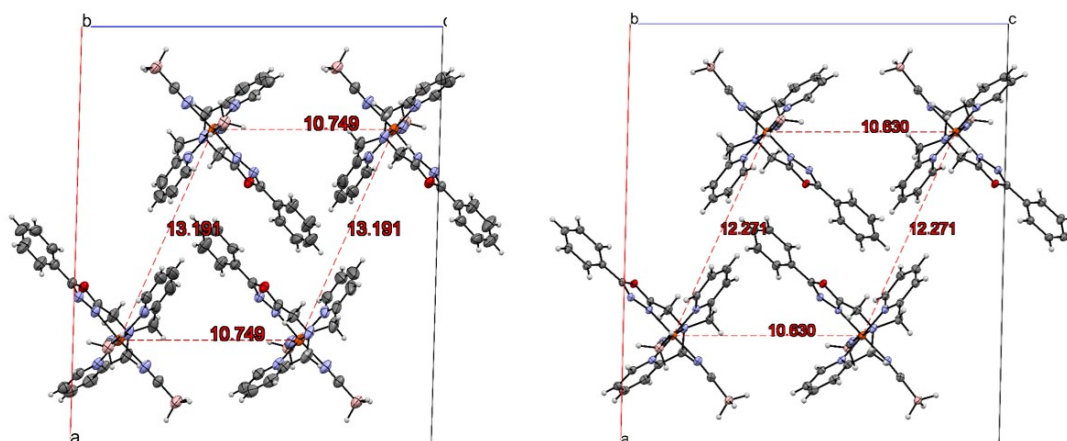


Figure S48: One-dimensional network of "complex dimers" in $[\text{Fe}_2(\text{L}^{\text{TetraPh-ODA}})(\text{NCBH}_3)] \cdot 1.5 \text{H}_2\text{O}$ (C6) at 240 K (left) and 120 K (right). Unit cell changes are remarkably more pronounced along the a-axis, which corresponds to the interdimer short contacts. Red dashed lines represent intermolecular distances between iron(II) centers. Colour scheme: pink – B, dark grey – C, grey – H, violet – N, red – O, orange – Fe. ORTEP representation with atomic displacement parameters set to 50 % probability.

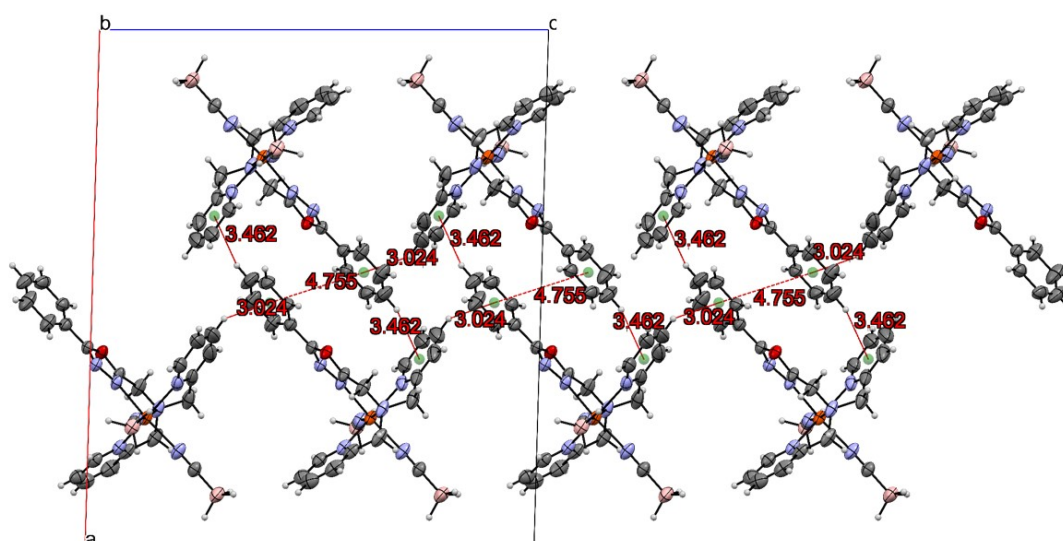


Figure S49: One-dimensional network of “complex dimers” in $[\text{Fe}_2^{\text{II}}(\text{L}^{\text{TetraPh-ODA}})(\text{NCBH}_3)] \cdot 1.5 \text{H}_2\text{O}$ (C6). Red dashed lines represent intermolecular distances. Colour scheme: pink – B, dark grey – C, grey – H, violet – N, red – O, orange – Fe. ORTEP representation with atomic displacement parameters set to 50 % probability.

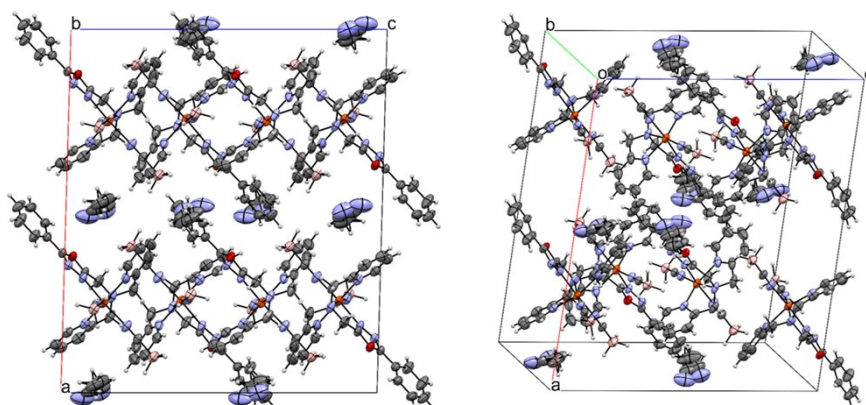


Figure S50: Unit cell of $[\text{Fe}_2^{\text{II}}(\text{L}^{\text{TetraPh-ODA}})(\text{NCBH}_3)] \cdot 1.5 \text{H}_2\text{O}$ (C6) (240 K) with view along the b-axis (left) and perspective view (right). ORTEP representation with atomic displacement parameters set to 50 % probability.

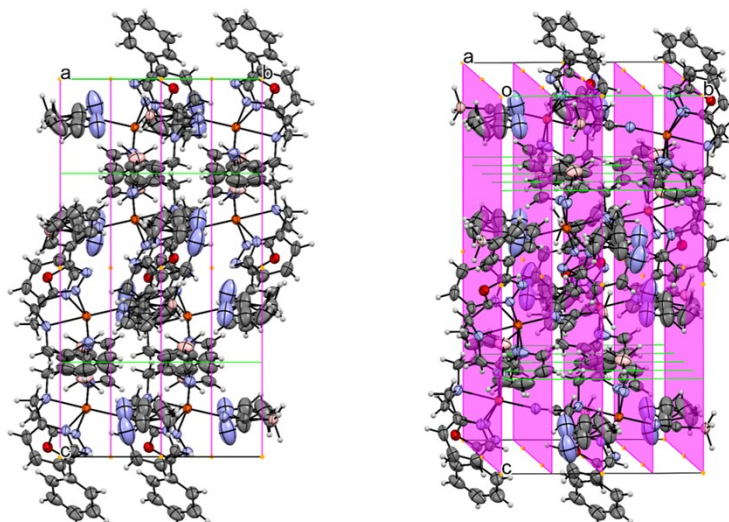


Figure S51: Unit cell of $[\text{Fe}_2^{\text{II}}(\text{L}^{\text{TetraPh-ODA}})(\text{NCBH}_3)] \cdot 1.5 \text{H}_2\text{O}$ (C6) (240 K) with present symmetry elements with view along the a-axis (left) and perspective view (right). Centres of Inversion – yellow dots, Two-fold Axis – green lines, Mirror Glide Planes – purple planes.

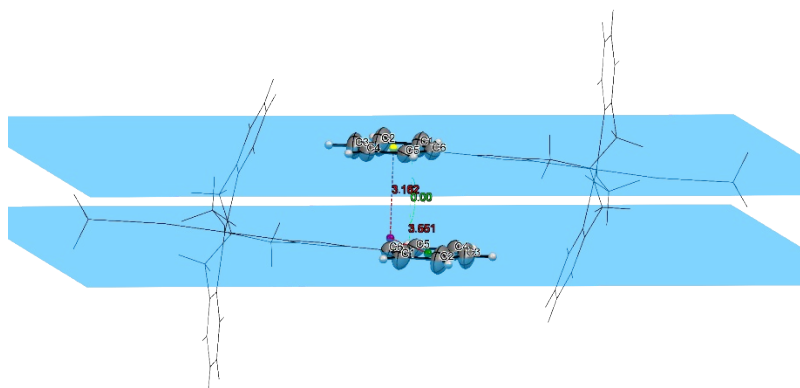


Figure S52: π - π interaction in $[\text{Fe}_2^{\text{II}}(\text{L}^{\text{TetraPh-ODA}})(\text{NCBH}_3)] \cdot 1.5 \text{H}_2\text{O}$ (C6) (240 K). Least-squares mean plane A is defined by C1, C2, C3, C4, C5 and C6. Plane B is defined by C1, C2, C3, C4, C5 and C6 of an adjacent molecule. Green point – centre of the aromatic ring in A. Yellow point – centre of the aromatic ring in B. Purple point –

orthogonal intersection of the aromatic centre in B onto plane A. Offset $r = 3.56 \text{ \AA}$, interplanar distance $d_{AB} = 3.16 \text{ \AA}$, interplanar angle $\vartheta = 0^\circ$. ORTEP representation with atomic displacement parameters set to 50 % probability.

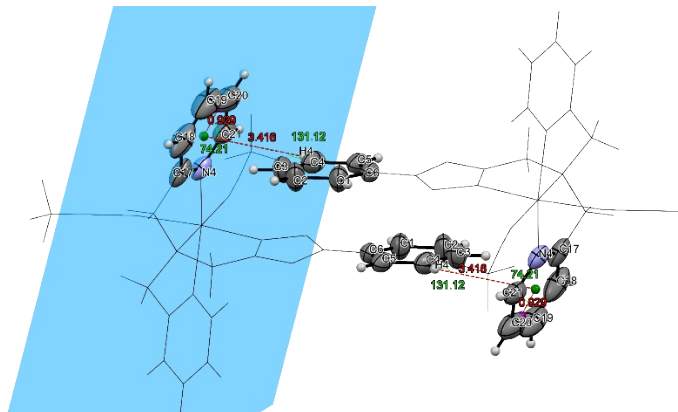


Figure S53: C-H ... π interaction in $[\text{Fe}_2^{\text{II}}(\text{L}^{\text{TetraPh-ODA}})(\text{NCBH}_3)] \cdot 1.5 \text{ H}_2\text{O}$ (**C6**) (240 K). Least-squares plane A is defined by N4, C17, C18, C19, C20 and C21. Interacting C-H fragment is labeled as C4-H4. Green point – centre of the aromatic ring in A. Purple point – orthogonal intersection of H19 onto plane A. Offset $r = 0.93 \text{ \AA}$, interaction distance $d_{\text{QH}} = 3.42 \text{ \AA}$, $\alpha = 131.1^\circ$ and $\beta = 74.2^\circ$. ORTEP representation with atomic displacement parameters set to 50 % probability.

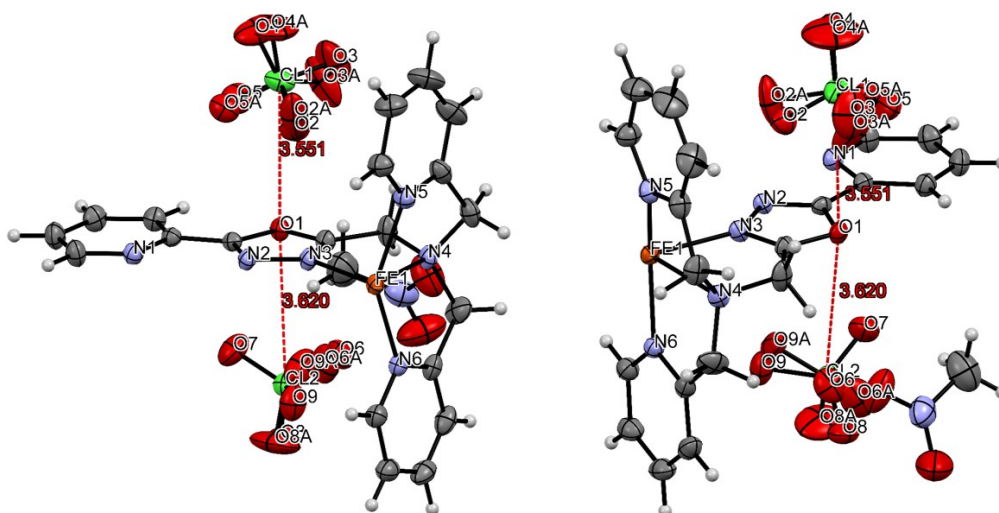


Figure S54: Asymmetric Unit of $[\text{Fe}_2^{\text{II}}(\text{L}^{\text{TetraPy}})](\text{ClO}_4)_4 \cdot \text{CH}_3\text{NO}_2 \cdot 1.5 \text{ H}_2\text{O}$ (**C6**) with different views. One perchlorate anion (Cl2O4) shows rotational disorder around its Cl2-O7 axis. The other perchlorate molecule (Cl1O4) exhibits disorder of its oxygen atoms between two positions in close proximity. ORTEP representation with atomic displacement parameters set to 50 % probability.

4. Cyclic Voltammetry:

To investigate the redox property of complex **C7**, cyclic voltammetry measurements were carried out in a TSC 1600 closed cell with an already built in platinum counter electrode as a vessel wall from rhd instruments. The working electrode was a glassy carbon electrode, which was polished before use with an aluminium oxide polishing paste with grain sizes of $0.1 \mu\text{m}$ FOR 30 minutes and $0.05 \mu\text{m}$ for an additional 20 minutes from Buehler on a

microfiber cloth. The electrodes were then washed with deionised water and acetonitrile and dried overnight at 60 C. For reference a silver pseudo reference electrode was used by all the potentials are referred to Fc/Fc⁺ by carrying out ferrocene run at the end. The conducting salt used was 0.1 M tetrabutylammonium hexafluorophosphate. The electrochemical property of complex **C7** was analysed in acetonitrile. The complex exhibit a single Fe(II)/Fe(III) redox event at $E_m = 0.8$ V versus Fc⁺/Fc, consistent with there being only one Fe(II) environment in these di-nuclear complex.

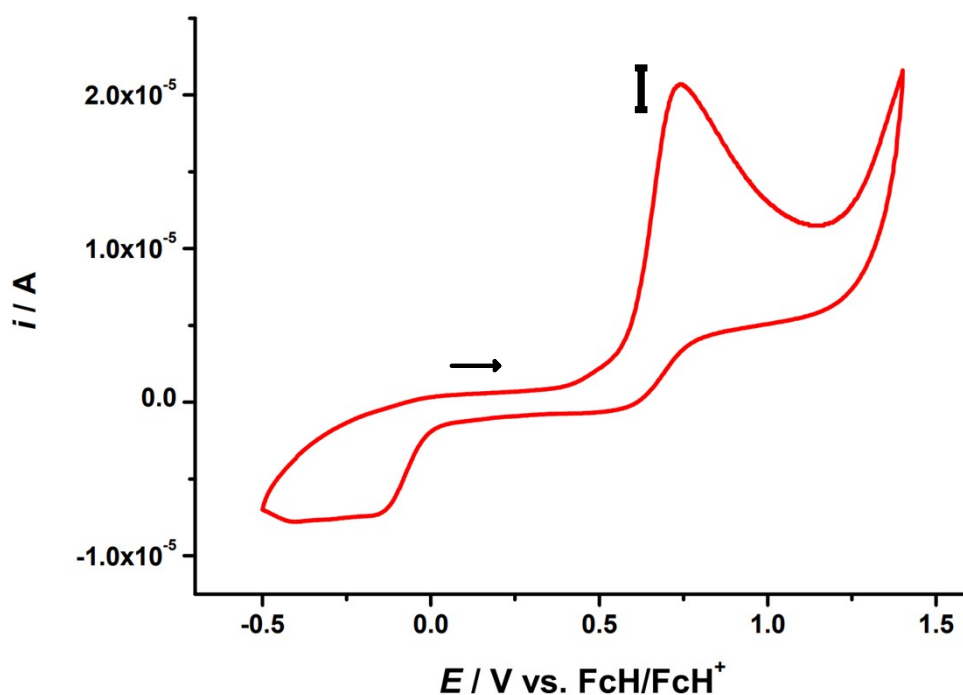


Figure S55: Cyclic voltammogram of $[\text{Fe}_2^{\text{II}}(\text{L}^{\text{TetraPy}})](\text{ClO}_4)_4 \cdot \text{CH}_3\text{NO}_2 \cdot 1.5 \text{H}_2\text{O}$ (**C6**) in 1mM solution of in MeCN (0.1 mol L⁻¹ TBAPF6 versus Fc⁺/Fc) at 100 mV s⁻¹.

5. Solid-State Magnetic Data:

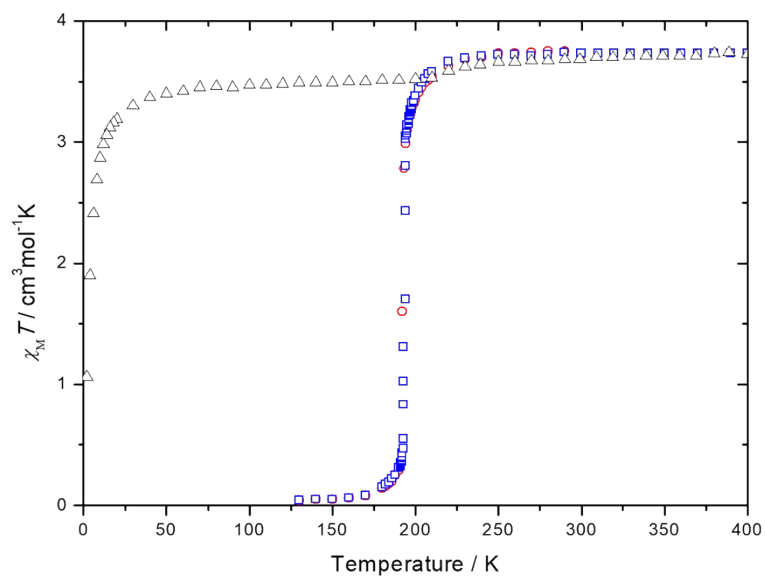


Figure S56: Temperature dependent magnetic behaviour of single crystals of $[\text{Fe}_2^{\text{II}}(\text{L}^{\text{TetraPh-ODA}})(\text{NCBH}_3)] \cdot X \text{ MeCN}$ (**C6**) in the form of a $\chi_M T$ vs. T plot. Measurement was done from 300-130 K (red open circles), 130-400 K (blue open squares) and 400-2 K (black open triangles).

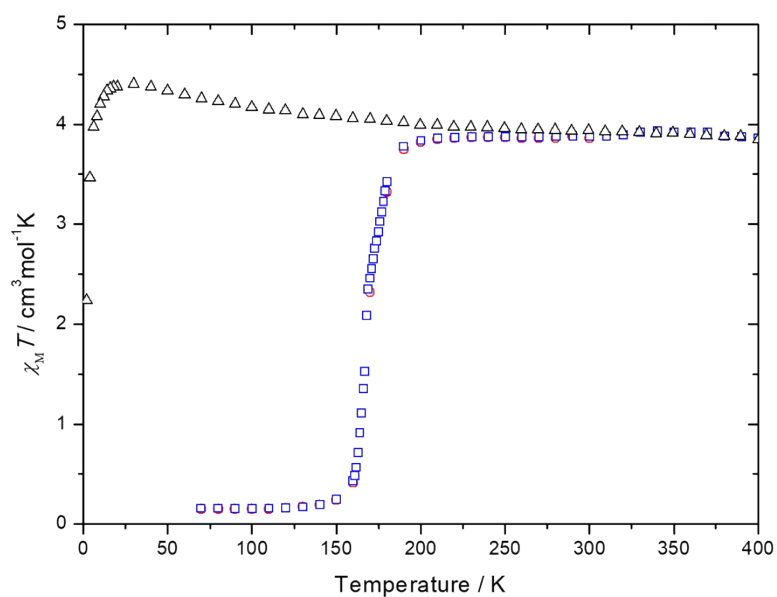


Figure S57: Temperature dependent magnetic behaviour of single crystals of $[\text{Fe}_2^{\text{II}}(\text{L}^{\text{TetraPy-ODA}})(\text{NCBH}_3)] \cdot X \text{ MeCN}$ (**C3**) in mother liquor in the form of a $\chi_M T$ vs. T plot. Measurement was done from 300-70 K (red open circles), 70-400 K (blue open squares) and 400-2 K (black open triangles).

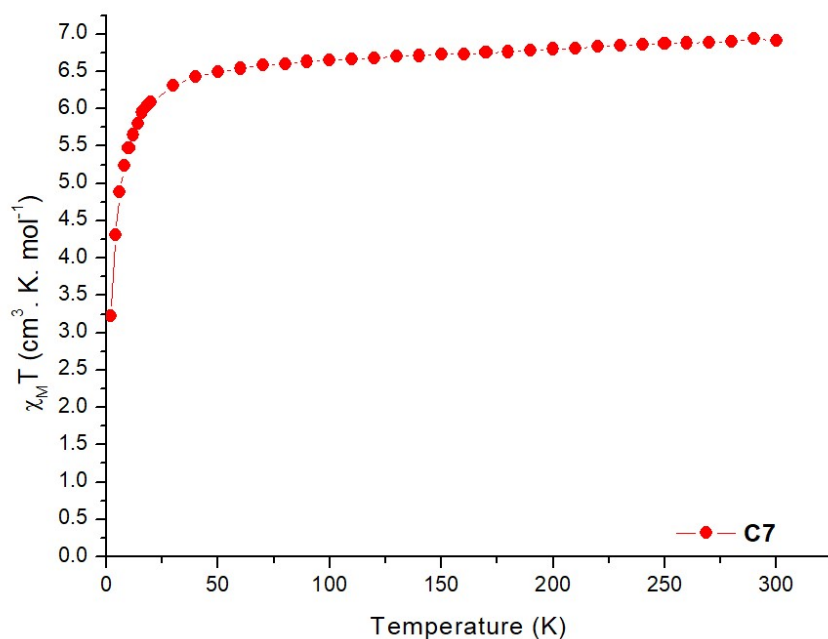


Figure S58: $\chi_M T$ vs T for complexes **C7**. The dots are the data points, and the line is just guide for the eye.

6. Computational details:

Table S6: The B3LYP computed structural parameters along with the X-ray parameters for complexes **C1-C6**.

Structural parameter	C1			Structural parameter	C2			Structural parameter	C3		
	EXP	HS	LS		EXP	HS	LS		EXP	HS	LS
Fe-N1	2.227	2.125	1.990	Fe-N3	2.204	2.140	2.204	Fe-N1	2.217	2.119	1.976
Fe-N4	2.295	2.362	2.077	Fe-N4	2.311	2.374	2.311	Fe-N4	2.281	2.353	2.080
Fe-N5	2.220	2.163	2.021	Fe-N5	2.170	2.166	2.170	Fe-N5	2.163	2.150	2.032
Fe-N6	2.204	2.211	1.842	Fe-N6	2.176	2.166	2.176	Fe-N6	2.173	2.150	2.032
Fe-N7	2.101	2.163	2.021	Fe-N7	2.062	1.913	2.062	Fe-N7	2.071	1.911	1.914
Fe-N8	2.030	1.875	1.834	Fe-N8	2.105	2.244	2.105	Fe-N8	2.137	2.184	1.980
Angle N6-Fe-N8	97.94	96.82	97.76	Angle N7-Fe-N8	95.41	94.47	95.82	Angle N7-Fe-N8	92.97	92.36	90.38
Structural parameter	C4			Structural parameter	C5			Structural parameter	C6		
	EXP	HS	LS		EXP	HS	LS		EXP	HS	LS
Fe-N2	2.184	2.147	1.985	Fe-N2	2.171	2.137	1.982	Fe-N2	1.965	1.995	1.974
Fe-N3	2.303	2.383	2.078	Fe-N3	2.294	2.376	2.075	Fe-N3	2.035	2.347	2.079
Fe-N4	2.210	2.165	2.019	Fe-N4	2.207	2.166	2.023	Fe-N5	1.970	2.062	2.032
Fe-N5	2.217	2.165	2.022	Fe-N5	2.205	2.166	2.021	Fe-N6	1.936	2.075	1.920
Fe-N6	2.058	1.876	1.839	Fe-N6	2.065	1.913	1.858	Fe-N7	1.952	2.347	1.979
Fe-N7	2.095	2.193	1.848	Fe-N7	2.091	2.243	1.868	Fe-N8	1.967	2.061	2.032
Angle N7-Fe-N6	96.34	92.46	98.21	Angle N6-Fe-N7	95.03	94.38	95.41	Angle N6-Fe-N7	89.85	93.70	89.73

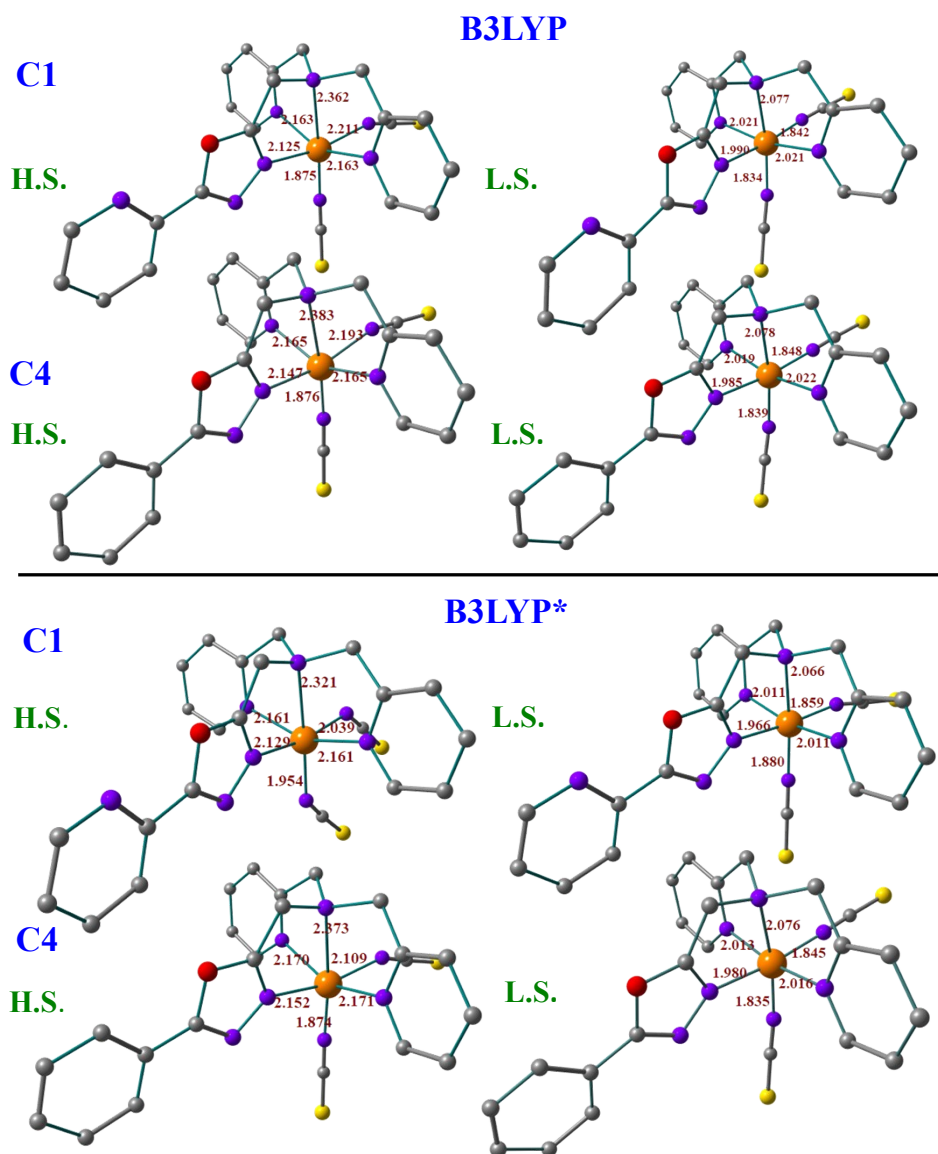


Figure S59: Optimized structure with B3LYP & B3LYP* hybrid functional along with some selected bond parameters for complexes **C1** and **C4**. Colour code: Orange = Fe (Iron), Purple = N (Nitrogen), Red = O (Oxygen), Grey = C (Carbon), Pale yellow = S (Sulfur) and hydrogen atoms are omitted for clarity.

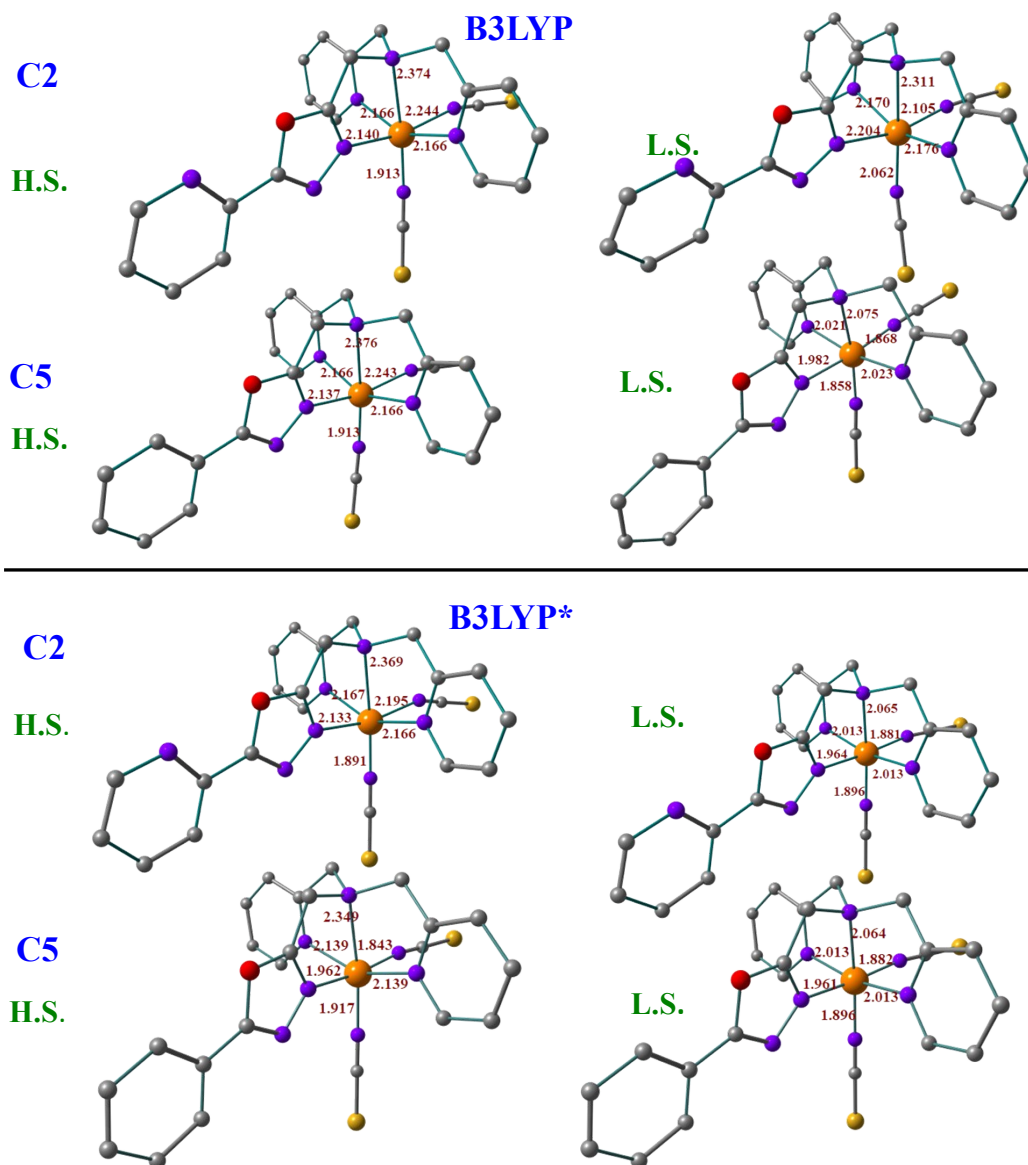


Figure S60: Optimized structure with B3LYP & B3LYP* hybrid functional along with some selected bond parameters for complexes **C2** and **C5**. Colour code: Orange = Fe (Iron), Purple = N (Nitrogen), Red = O (Oxygen), Grey = C (Carbon), Yellow = Se (Selenium), and hydrogen atoms are omitted for clarity.

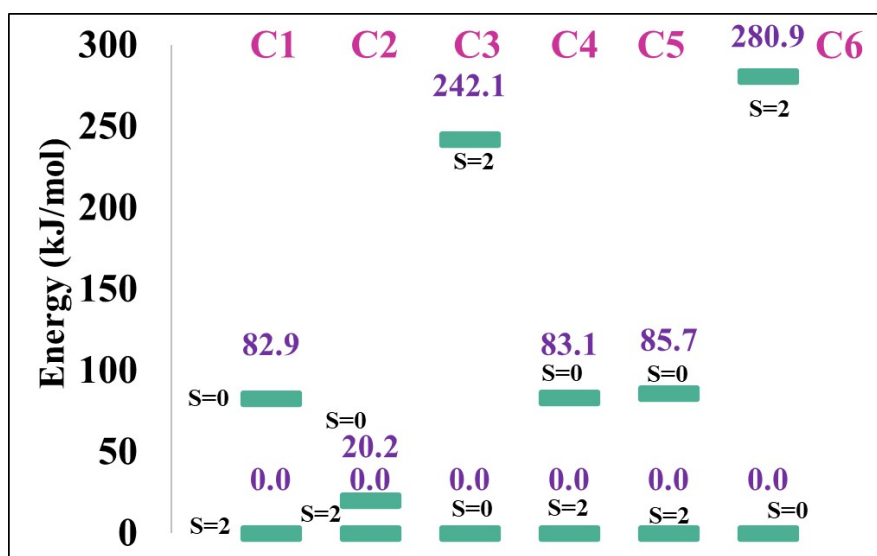


Figure S61: Energy difference in kJ/mol between two spin states computed with B3LYP for all six complexes.

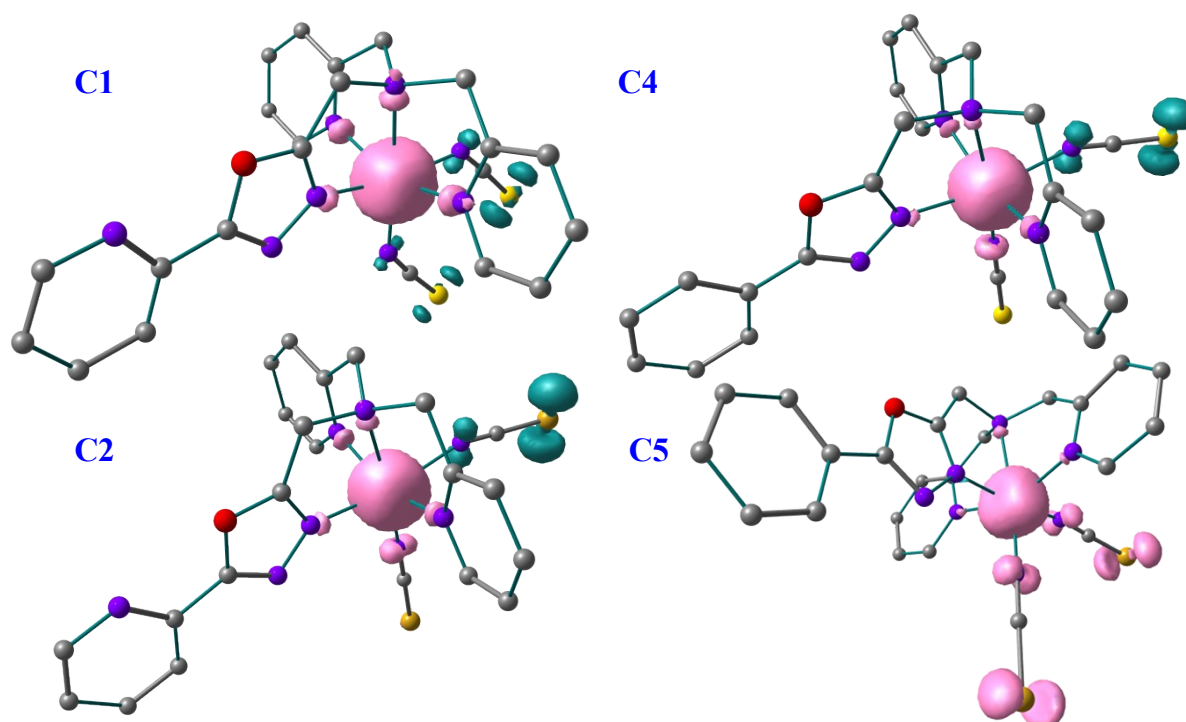


Figure S62: Spin density diagram for complex **C1**, **C2**, **C4**, and **C5** in High Spin state with B3LYP* optimized geometry.

7. References:

1. Alvarez, S.; Alemany, P.; Casanova, D.; Cirera, J.; Llunell, M.; Avnir, D. Continuous symmetry measures: A new tool in quantum chemistry. *Coord. Chem. Rev.* **2005**, *249*, 1693–1708.